UNLIMITED DISTRIBUTION

National Defence / Défense nationale
Research and Development Branch / Bureau de recherche et développement

TECHNICAL MEMORANDUM 88/213
October 1988

ESTIMATES FOR THE ADDED MASS OF A MULTI-COMPONENT, DEEPLY SUBMERGED VEHICLE

PART I: Theory and Program Description

George D. Watt

Defence Research Establishment Atlantic
Centre de Recherches pour la Défense Atlantique

Canada

UNLIMITED DISTRIBUTION

National Defence
Research and Development Branch

Défense nationale
Bureau de recherche et développement

ESTIMATES FOR THE ADDED MASS OF A MULTI-COMPONENT, DEEPLY SUBMERGED VEHICLE
PART I: Theory and Program Description

George D. Watt

October 1988

Approved by L.J.Leggat Director/Technology Division

DISTRIBUTION APPROVED BY

D/TD

TECHNICAL MEMORANDUM 88/213

Defence Research Establishment Atlantic

Centre de Recherches pour la Défense Atlantique

Canada

Abstract

An analytic method is presented for estimating all the added mass terms of a deeply submerged, submarine like, rigid body. This body may consist of any number of components (hull, sail, fins, etc.). Each component is represented by an ellipsoid with three independently sized principal axes; this allows the added masses to be calculated analytically. Ellipsoid geometry, orientation, and relative location are chosen so that both added masses and added moments of inertia are optimally modelled. Interference effects between the main hull component and an appendage are approximately accounted for by using the flow field around a replacement ellipsoid for the hull to modify the flow at the appendage; interference effects between appendages are neglected. The analysis uses incompressible potential flow theory. It does not account for any circulation in the flow.

Calculations carried out using this method are very fast. They show that both appendage thickness and hull interference can appreciably affect those added mass coefficients which contribute to coupling.

Résumé

On présente une méthode analytique pour estimer tous les termes de masse ajoutée dans un corps rigide, ressemblant à un sous-marin, immergé en profondeur. Ce corps peut comporter un nombre quelconque de composantes (coque, riosque, ailerons, etc.). Chaque composante est représentée par une ellipsoide possédant trois axes principaux de longueurs indépendantes, ce qui permet de calculer les masses ajoutées de façon analytique. La forme, l'orientation et la position relative des ellipsoides sont choisies de façon que les masses et moments d'inertie ajoutés sont modélisés de façon optimale. L'interférence entre la composante principale, la coque, et un ajout est approchée par l'application d'un champ d'écoulement autour d'une ellipsoide de remplacement de la coque qui modifie l'écoulement autour de l'ajout; l'interférence entre des ajouts n'est pas pris en compte. L'analyse s'appuie sur la théorie de l'écoulement de potentiel incompressible qui n'admet aucune circulation dans l'écoulement.

Les calculs effectués par cette méthode sont très rapides. Ils révèlent que l'épaisseur de l'jout et l'interférence de la coque peuvent influer beaucoup sur les coefficients de masse ajoutée qui contribuent au couplage.

Contents

Nomenclature

a, b, c	half the lengths of an ellipsoid's principal axes oriented along the x', y', z' axes, respectively.
$\mathbf{A}$	the matrix transforming a vector description given relative to inertial x_0, y_0, z_0 axes to its description in body fixed x, y, z axes.
$B(x)$	the breadth of a hull component as a function of longitudinal position; this profile is assumed to be symmetrical about its centerline.
$\mathbf{B}$	the matrix transforming a vector description given relative to body fixed x, y, z axes to its description relative to the ellipsoidal principal axes, x', y', z'.
$c_1, c_2, \ldots, c_5$	appendage chord lengths measured parallel to the x' axis; see Figure 2.
E, E'	complete elliptic integrals of the second kind.
$E(u)$	incomplete elliptic integral of the second kind.
$\mathbf{F}$	interference matrix containing the interference velocities at a secondary component.
$H(x)$	the height of a hull component as a function of longitudinal position; this component is not assumed to be symmetrical about its centerline.
$\overline{H}(x)$	the z coordinate of the midpoint of the local height.
$\mathbf{i}, \mathbf{j}, \mathbf{k}$	unit vectors associated with the x, y, z body fixed axes.
k, k'	modulus and complementary modulus of elliptic functions.
$K,\ K' = \frac{K}{\frac{1}{2}\rho U^2 \ell^3}$	rolling moment and dimensionless rolling moment on vehicle; moment is about body fixed x axis.
$K_{\dot{u}}, K_{\dot{v}}, K_{\dot{w}}$	added mass coefficients giving the linear variation of rolling moment with $\dot{u}, \dot{v}, \dot{w}$.
$K'_{\dot{u}}, K'_{\dot{v}}, K'_{\dot{w}}$	added mass coefficients nondimensionlized by $\frac{1}{2}\rho\ell^4$; eg, $K'_{\dot{u}} = K_{\dot{u}}/\frac{1}{2}\rho\ell^4$.
$K_{\dot{p}}, K_{\dot{q}}, K_{\dot{r}}$	added mass coefficients giving the linear variation of rolling moment with $\dot{p}, \dot{q}, \dot{r}$.
$K'_{\dot{p}}, K'_{\dot{q}}, K'_{\dot{r}}$	added mass coefficients nondimensionalized by $\frac{1}{2}\rho\ell^5$; eg, $K'_{\dot{p}} = K_{\dot{p}}/\frac{1}{2}\rho\ell^5$.
K, K'	complete elliptic integrals of the first kind.
ℓ	length of the vehicle.
$M,\ M' = \frac{M}{\frac{1}{2}\rho U^2 \ell^3}$	pitching moment and dimensionless pitching moment on vehicle; moment is about body fixed y axis.

$M_{\dot{u}}, M_{\dot{v}}, M_{\dot{w}}$	added mass coefficients giving the linear variation of pitching moment with $\dot{u}, \dot{v}, \dot{w}$.
$M'_{\dot{u}}, M'_{\dot{v}}, M'_{\dot{w}}$	added mass coefficients nondimensionlized by $\frac{1}{2}\rho\ell^4$; eg, $M'_{\dot{u}} = M_{\dot{u}}/\frac{1}{2}\rho\ell^4$.
$M_{\dot{p}}, M_{\dot{q}}, M_{\dot{r}}$	added mass coefficients giving the linear variation of pitching moment with $\dot{p}, \dot{q}, \dot{r}$.
$M'_{\dot{p}}, M'_{\dot{q}}, M'_{\dot{r}}$	added mass coefficients nondimensionlized by $\frac{1}{2}\rho\ell^5$; eg, $M'_{\dot{p}} = M_{\dot{p}}/\frac{1}{2}\rho\ell^5$.
$\mathbf{M}$	matrix transforming velocities and angular velocities specified relative to body axes to a representation relative to ellipsoid principal axes, see equation 17.
$N,\ N' = \frac{N}{\frac{1}{2}\rho U^2 \ell^3}$	yawing moment and dimensionless yawing moment on vehicle; moment is about body fixed z axis.
$N_{\dot{u}}, N_{\dot{v}}, N_{\dot{w}}$	added mass coefficients giving the linear variation of yawing moment with $\dot{u}, \dot{v}, \dot{w}$.
$N'_{\dot{u}}, N'_{\dot{v}}, N'_{\dot{w}}$	added mass coefficients nondimensionlized by $\frac{1}{2}\rho\ell^4$; eg, $N'_{\dot{u}} = N_{\dot{u}}/\frac{1}{2}\rho\ell^4$.
$N_{\dot{p}}, N_{\dot{q}}, N_{\dot{r}}$	added mass coefficients giving the linear variation of yawing moment with $\dot{p}, \dot{q}, \dot{r}$.
$N'_{\dot{p}}, N'_{\dot{q}}, N'_{\dot{r}}$	added mass coefficients nondimensionlized by $\frac{1}{2}\rho\ell^5$; eg, $N'_{\dot{p}} = N_{\dot{p}}/\frac{1}{2}\rho\ell^5$.
p, q, r	vehicle angular velocities resolved about the body fixed x, y, z axes, respectively.
p', q', r'	body component angular velocities resolved about its replacement ellipsoid's x', y', z' axes, respectively.
q, q'	theta function parameters; purely functions of k and k'.
q_j	a generalized coordinate in the Lagrangian equations of motion.
Q_j	the force associated with the generalized coordinate q_j in the Lagrangian equations of motion.
	displacement vector, using a body axes representation, giving the location of the centroid of a component's replacement ellipsoid: $\bar{x}\mathbf{i} + \bar{y}\mathbf{j} + \bar{z}\mathbf{k}$.
t	thickness to chord ratio for an appendage.
$t_{11}, t_{22}, \ldots, t_{66}$	inertia coefficients determining the kinetic energy of an ellipsoid moving through an ideal fluid with six degrees of freedom; t_{11} is associated with translation along the x' axis, t_{22} with translation along the y' axis, ..., t_{66} with rotation about the z' axis.
$t'_{11}, t'_{22}, \ldots, t'_{66}$	inertia coefficients as above, except that t'_{11} is associated with translation along the longest of the ellipsoid principal axes, t'_{22} with translation along the second longest principal axis, ..., t'_{66} with rotation about the shortest principal axis.

T	the kinetic energy in an ideal fluid.
u, v, w	translational velocities of the vehicle resolved along the body fixed x, y, z axes, respectively.
u', v', w'	translational velocities of the centroid of a body component's replacement ellipsoid resolved along its x', y', z' axes, respectively.
u	argument of the Jacobian elliptic functions.
U	speed of the vehicle: $\sqrt{u^2 + v^2 + w^2}$.
$\mathbf{v}_0, \mathbf{v}, \mathbf{v}'$	translational velocity vectors using inertial, body fixed, and ellipsoid principal axes representations, respectively.
V	volume of an ellipsoid: $\frac{4}{3}\pi abc$.
x_0, y_0, z_0	set of inertial axes, fixed in space.
x, y, z	axes fixed in the body of the vehicle: the x axis points forward, the y axis points to starboard, and the z axis points through the keel; the orientation of these axes relative to the inertial axes is given by the angles ψ, θ, and ϕ.
$\bar{x}, \bar{y}, \bar{z}$	body fixed coordinates locating the centroid of a replacement ellipsoid.
x', y', z'	axes aligned with the principal axes of a body component's replacement ellipsoid, such that their origins coincide with the centroid of the ellipsoid; their orientation relative the body fixed axes is defined by the angles Φ and Ω.
$\hat{x}, \hat{y}, \hat{z}$	an intermediate set of axes between the x, y, z and x', y', z' axes used for describing the geometry of an appendage, as shown in Figure 2; their orientation relative to the body fixed axes is defined by the angle Φ.
$X,\ X' = \frac{X}{\frac{1}{2}\rho U^2 \ell^2}$	axial force and dimensionless axial force on the vehicle; force is in the x direction.
$X_{\dot{u}}, X_{\dot{v}}, X_{\dot{w}}$	added mass coefficients giving the linear variation of axial force with $\dot{u}, \dot{v}, \dot{w}$.
$X'_{\dot{u}}, X'_{\dot{v}}, X'_{\dot{w}}$	added mass coefficients nondimensionlized by $\frac{1}{2}\rho\ell^3$; eg, $X'_{\dot{u}} = X_{\dot{u}}/\frac{1}{2}\rho\ell^3$.
$X_{\dot{p}}, X_{\dot{q}}, X_{\dot{r}}$	added mass coefficients giving the linear variation of axial force with $\dot{p}, \dot{q}, \dot{r}$.
$X'_{\dot{p}}, X'_{\dot{q}}, X'_{\dot{r}}$	added mass coefficients nondimensionlized by $\frac{1}{2}\rho\ell^4$; eg, $X'_{\dot{p}} = X_{\dot{p}}/\frac{1}{2}\rho\ell^4$.
$Y,\ Y' = \frac{Y}{\frac{1}{2}\rho U^2 \ell^2}$	lateral force and dimensionless lateral force on the vehicle; force is in the y direction.
$Y_{\dot{u}}, Y_{\dot{v}}, Y_{\dot{w}}$	added mass coefficients giving the linear variation of lateral force with $\dot{u}, \dot{v}, \dot{w}$.
$Y'_{\dot{u}}, Y'_{\dot{v}}, Y'_{\dot{w}}$	added mass coefficients nondimensionlized by $\frac{1}{2}\rho\ell^3$; eg, $Y'_{\dot{u}} = Y_{\dot{u}}/\frac{1}{2}\rho\ell^3$.

$Y_{\dot{p}}, Y_{\dot{q}}, Y_{\dot{r}}$	added mass coefficients giving the linear variation of lateral force with $\dot{p}, \dot{q}, \dot{r}$.
$Y'_{\dot{p}}, Y'_{\dot{q}}, Y'_{\dot{r}}$	added mass coefficients nondimensionlized by $\frac{1}{2}\rho\ell^4$; eg, $Y'_{\dot{p}} = Y_{\dot{p}}/\frac{1}{2}\rho\ell^4$.
$Z,\ Z' = \frac{Z}{\frac{1}{2}\rho U^2\ell^2}$	normal force and dimensionless normal force on the vehicle; force is in the z direction.
$Z_{\dot{u}}, Z_{\dot{v}}, Z_{\dot{w}}$	added mass coefficients giving the linear variation of normal force with $\dot{u}, \dot{v}, \dot{w}$.
$Z'_{\dot{u}}, Z'_{\dot{v}}, Z'_{\dot{w}}$	added mass coefficients nondimensionlized by $\frac{1}{2}\rho\ell^3$; eg, $Z'_{\dot{u}} = Z_{\dot{u}}/\frac{1}{2}\rho\ell^3$.
$Z_{\dot{p}}, Z_{\dot{q}}, Z_{\dot{r}}$	added mass coefficients giving the linear variation of normal force with $\dot{p}, \dot{q}, \dot{r}$.
$Z'_{\dot{p}}, Z'_{\dot{q}}, Z'_{\dot{r}}$	added mass coefficients nondimensionlized by $\frac{1}{2}\rho\ell^4$; eg, $Z'_{\dot{p}} = Z_{\dot{p}}/\frac{1}{2}\rho\ell^4$.
$\alpha_0, \beta_0, \gamma_0$	constants used in the velocity potentials for flow around an ellipsoid.
λ, μ, ν	confocal ellipsoidal coordinates; λ = constant defines the surface of an ellipsoid.
μ, ν	an intermediate set of axes between the x, y, z and x', y', z' axes used in calculating the replacement ellipsoid geometry for an appendage; see Figure 2.
μ, ν	coordinates giving the centroid of a replacement ellipsoid using the μ, ν axes of Figure 2.
ξ, σ, τ	the largest, second largest, and smallest, respectively, of a, b, c.
ρ	fluid density.
Φ, Ω	the roll and sweepback angles, respectively, of the x', y', z' axes relative to the body fixed x, y, z axes.
φ	velocity potential in the inertial reference frame: $\mathbf{v}_0 = -\nabla\varphi$.
$\varphi_1, \varphi_2, \ldots, \varphi_6$	velocity potentials giving the potential flow around an ellipsoid in each of the six degrees of freedom.
$\chi_1, \chi_2, \ldots, \chi_6$	those parts of the above velocity potentials which are purely functions of λ.
ψ, θ, ϕ	the yaw, pitch, and roll angles, respectively, of the body fixed x, y, z axes relative to the inertial x_0, y_0, z_0 axes.
$\omega_0, \omega, \omega'$	angular velocity vectors using inertial, body fixed, and ellipsoid principal axes representations, respectively.

1 Introduction

DREA is currently developing the ability to model the maneuvering characteristics of submarines. This will enable the evaluation of proposed candidates for the Canadian Submarine Acquisition Program and, in the longer term, provide the basis for a more detailed analysis of the dynamic performance of the new boats. The initial analysis package will be based on a numerical integration of the six nonlinear ordinary differential equations describing the motion in six degrees of freedom of a maneuvering vehicle. These equations are formulated using either theoretically or experimentally determined hydrodynamic coefficients.

This memorandum presents a method for theoretically estimating one class of hydrodynamic coefficient, the acceleration coefficients — otherwise known as the added masses. It is the background report to Reference 1 and gives the complete details of the theory. For the convenience of the reader, it includes everything presented in Reference 1.

Added mass coefficients (added mass is taken to include added moments of inertia) receive their name because they can be linearly combined with the true submarine masses in the equations of motion to form one coefficient. Mathematically, added mass is just the proportionality constant relating the kinetic energy in the fluid surrounding the vehicle to the square of the vehicle's speed, in the same way that vehicle mass relates vehicle kinetic energy to speed squared. During vehicle accelerations, both the kinetic energy of the vehicle and the fluid are changed, their ratio remaining constant in an ideal fluid. Therefore, an accelerating vehicle must overcome the effective inertia of both vehicle mass and 'added mass'. The added masses for a submarine can be equivalent in magnitude to the actual submarine masses, and so must be accounted for properly.

It is generally acknowledged that submarine added mass coefficients, insofar as they are important in the equations of motion, are not strongly dependent on viscous effects (such as circulation and boundary layer growth). Indeed, many of the experimental techniques currently in use for determining the coefficients make this assumption since they ignore the dependence of added mass on both orientation of the vehicle to the oncoming flow, and time in an unsteady flow (stationary model oscillations assume this, for example). The assumption is also consistent with most modern formulations of the equations of motion in which each added mass coefficient is assumed to be a constant. Theoretically, these assumptions are false given the vortex structures known to exist and the lifting surface Kutta conditions that must be met in the flow; however, while these flow phenomena frequently dominate the steady state flow field resulting from a sudden or violent maneuver, they are often not present at the beginning of the maneuver when vehicle accelerations are largest. All things considered, a potential flow analysis, neglecting circulation, is an appropriate method for estimating the added mass coefficients. If it is found necessary to account for flow structures and circulation effects in a particular application, then the equations of motion will need to be reformulated to allow the added mass coefficients to vary with the state variables.

There are various potential flow methods available for predicting the added masses, including exact-numerical solutions of the flow about the complete vehicle configuration. However, a simple approach resulting in quick calculation times is most appropriate in view of the approximations discussed above.

A submarine's hull is generally responsible for the greatest contribution to the added mass coefficients. Hull coefficients are often obtained by representing the hull with an ellipsoid. This is convenient because of the availability of exact analytical potentials, derived by Lamb[2],

describing the flows and giving the added masses for ellipsoids moving in six degrees of freedom. Imlay[3] has interpreted Lamb's work in terms of a symmetrically finned prolate spheriod (ie, an axisymmetric submarine without a sail); he summarizes the added mass expressions and discusses their use in the general ideal expressions for the equations of motion.

Humphreys and Watkinson[4] give a comprehensive summary of the usual formulae used for estimating the added masses of a multi-component vehicle; they include a good discussion of how important each term is to the equations of motion (sensitivity studies). To simplify the analysis, submarine configurations are broken down to their constituent components, such as hull, sail, and fins. The added masses of each component are calculated separately and then summed with those of the other components to give the configuration added masses. Hull added masses are obtained by replacing the hull with an axisymmetric ellipsoid. Appendage added masses are calculated semi-empirically using flat plate models. The Humphreys and Watkinson sensitivity studies show these procedures give adequate accuracy. However, Humphreys and Watkinson do not deal at length with asymmetrical hull shapes or configurations with sails, and the sail, in particular, can have large effects on those coefficients which contribute to coupling between motions in different degrees of freedom. Aucher[5] estimates added masses in a similar fashion. Neither of these methods account for any hull asymmetry. Instead, they model the hull with an axisymmetric ellipsoid whose geometry is determined by an average hull diameter.

Another approach[6] uses strip theory to estimate hull coefficients. Here, two-dimensional, potential, cross-flow predictions estimate the local added mass per unit length at a longitudinal location; these local contributions are then integrated over the length of the hull to give its added masses. Although able to account for hull asymmetries, strip theory leads to an overprediction of the principal added mass coefficients (relative to an exact 3-D potential flow solution) of from 5 to 15 percent, depending on the coefficient and hull geometry. Empirical corrections can be applied, but they are data base dependent.

The approach taken in the present theory is to combine and extend the above procedures and, as far as is possible, apply the ideal equations of motion in a manner that estimates all the added mass coefficients of the vehicle as accurately as possible. For maximum flexibility, each body component is represented by an ellipsoid with three independently sized principal axes. The ellipsoid is positioned and oriented so that both added masses and added moments of inertia are modelled properly. As with previous theories, the total added masses of the vehicle are taken to be the sum of the added masses of each of the component ellipsoids, except that interference effects between the hull and appendages are accounted for first. These effects can be appreciable, changing an appendage's added mass contribution by as much as 50 to 100 percent relative to a calculation which assumed the appendage was isolated in the flow. The present theory approximately accounts for this by using the flow field around a replacement ellipsoid for the hull to modify the flow at the appendage. Interference effects between appendages are neglected.

Special attention is given to choosing the geometry of the hull replacement ellipsoid. This is done by

1) calculating strip theory added mass predictions from specified hull coordinates, and then
2) choosing ellipsoid geometry in such a way that strip theory predictions generated from the ellipsoid coordinates agree as well as possible with the hull strip theory predictions.

Thus, the hull replacement ellipsoid models those geometrical characteristics of the hull which are most important in determining added mass. The added masses for the hull are obtained by applying Lamb's theory to this ellipsoid; they can be thought of as strip theory predictions automatically (though approximately) accounting for 3-D effects .

Appendages have only a small effect on the principal added masses associated with translation and rotation in the transverse directions, but can appreciably affect and even dominate those coefficients associated with surge and roll. Appendages are also important to the so-called 'off-diagonal' added mass coefficients which, though smaller in magnitude than the diagonal terms, are potentially important as coupling mechanisms. Representing an appendage with an ellipsoid, while less satisfactory than the hull representation, is considered an appropriate approximation given the small contribution the appendage will make to the vehicle's dominant coefficients. Doing so also allows appendage thickness to be accounted for, and this is shown to have appreciable effects on some of the coefficients.

Significantly, ellipsoid potential flow solutions, and the added mass expressions they generate, require the evaluation of elliptic functions if the ellipsoids have three independently sized principal axes. This explains the approximation usually made to avoid these calculations: by replacing the hull with an axisymmetric ellipsoid, only elementary functions need be evaluated. For the present theory, fast, accurate, analytically oriented routines are derived for evaluating the requisite elliptic functions.

A computer program has been written to calculate the predictions of the theory developed in this report; its use is described in Appendix B. In Section 10, the theory is applied to a generic submarine configuration and results are presented.

2 The Equations of Motion of an Ideal Fluid

Although some of the relationships developed in this section have been presented by other authors (Lamb[2], Imlay[3], Abkowitz[7]), it is felt that a thorough and complete presentation collated in one place is desirable. This also allows the reader to more easily follow the extensions that are made to the above theories.

By deriving the equations of motion of the fluid around the vehicle, expressions for the ideal fluid forces exerted on the vehicle can be obtained. One begins by establishing coordinate systems and a set of variables describing the motion.

Consider the unsteady motion of a vehicle in six degrees of freedom having arbitrary translational and rotational velocities. In order to describe the motion, it is conventional[8] to use a set of body fixed axes, x, y, z, which move with velocities u, v, w in the x, y, z directions relative to a set of inertial axes x_0, y_0, z_0. The angular velocity components of the body about the x, y, z axes are p, q, r. Take the x_0, y_0 axes to be in the horizontal plane and the z_0 axis to point downwards. For a submarine, the x axis points forward, the y axis to starboard, and the z axis through the keel.

To describe the orientation of the body axes relative to the inertial axes, angles of yaw (ψ), pitch (θ), and roll (ϕ) are defined in the following way[7]. Since finite rotations of yaw, pitch, and roll in any order do *not* result in the same relative body axes orientation, the order of the rotations is an integral part of the definitions of the angles. Assuming the body axes are initially aligned with the inertial axes (however much the origins are displaced), an arbitrary reorientation relative to the inertial axes is obtained by

1) yawing about the z axis through an angle ψ,

2) pitching about the y axis through an angle θ, and

3) rolling about the x axis through an angle ϕ.

All rotations are in the positive sense as defined by the Right Hand Rule. Thus, the matrix $\mathbf{A}$ transforming a vector description using x_0, y_0, z_0 axes to one using body axes is:

$$\mathbf{A} \equiv \mathbf{A}_\phi \mathbf{A}_\theta \mathbf{A}_\psi \equiv \begin{pmatrix} 1 & 0 & 0 \\ 0 & \cos\phi & \sin\phi \\ 0 & -\sin\phi & \cos\phi \end{pmatrix} \begin{pmatrix} \cos\theta & 0 & -\sin\theta \\ 0 & 1 & 0 \\ \sin\theta & 0 & \cos\theta \end{pmatrix} \begin{pmatrix} \cos\psi & \sin\psi & 0 \\ -\sin\psi & \cos\psi & 0 \\ 0 & 0 & 1 \end{pmatrix}$$

$$= \begin{pmatrix} \cos\theta\cos\psi & \cos\theta\sin\psi & -\sin\theta \\ -\sin\psi\cos\phi + \sin\phi\sin\theta\cos\psi & \cos\phi\cos\psi + \sin\phi\sin\theta\sin\psi & \sin\phi\cos\theta \\ \sin\phi\sin\psi + \cos\phi\cos\psi\sin\theta & -\sin\phi\cos\psi + \cos\phi\sin\theta\sin\psi & \cos\phi\cos\theta \end{pmatrix}. \quad (1)$$

Therefore, if $\mathbf{v}$ and $\mathbf{v}_0$ are the vectors specifying the velocity of the vehicle using body axes and inertial axes coordinate systems, respectively:

$$\mathbf{v} \equiv \begin{pmatrix} u \\ v \\ w \end{pmatrix}, \quad \mathbf{v}_0 \equiv \begin{pmatrix} \dot{x}_0 \\ \dot{y}_0 \\ \dot{z}_0 \end{pmatrix} \quad (2)$$

then:

$$\mathbf{v} = \mathbf{A}\mathbf{v}_0 \quad \text{and} \quad \mathbf{v}_0 = \mathbf{A}^{-1}\mathbf{v}. \quad (3)$$

Since $\mathbf{A}$ is an orthogonal matrix, $\mathbf{A}^{-1} = \mathbf{A}^{\mathrm{T}}$ (where $\mathbf{A}^{\mathrm{T}}$ is the *transpose* of $\mathbf{A}$).

Similarly, if ω and ω_0 are the angular velocity vectors giving the vehicle's rotation, then:

$$\omega = \mathbf{A}\,\omega_0 \quad \text{and} \quad \omega_0 = \mathbf{A}^{\mathrm{T}}\omega. \quad (4)$$

However, because of their definitions, $\dot{\psi}$, $\dot{\theta}$, and $\dot{\phi}$ do not form the orthogonal components for either of these vectors. The expression for ω is obtained by summing the contributions from $\dot{\psi}$, $\dot{\theta}$, and $\dot{\phi}$ after properly transforming their associated angular velocity vectors to a body axes representation:

$$\omega \equiv \begin{pmatrix} p \\ q \\ r \end{pmatrix} = \mathbf{A}_\phi \mathbf{A}_\theta \mathbf{A}_\psi \begin{pmatrix} 0 \\ 0 \\ \dot{\psi} \end{pmatrix} + \mathbf{A}_\phi \mathbf{A}_\theta \begin{pmatrix} 0 \\ \dot{\theta} \\ 0 \end{pmatrix} + \mathbf{A}_\phi \begin{pmatrix} \dot{\phi} \\ 0 \\ 0 \end{pmatrix}. \quad (5)$$

Thus:

$$\begin{aligned} p &= -\sin\theta\,\dot{\psi} + \dot{\phi} \\ q &= \sin\phi\cos\theta\,\dot{\psi} + \cos\phi\,\dot{\theta} \\ r &= \cos\phi\cos\theta\,\dot{\psi} - \sin\phi\,\dot{\theta}. \end{aligned} \quad (6)$$

Now, since our interest is only in the overall forces on the vehicle, which are equal and opposite to those on the fluid surrounding it, Lagrange's equations of motion in terms of the total energy in the flow field can be used. This description uses *generalized coordinates* (one for each degree of freedom), all of which must be independent. The generalized coordinates

used in this problem will be taken to be $x_0, y_0, z_0, \psi, \theta, \phi$; so that u, v, w, p, q, r are dependent variables related to the generalized coordinates via equations 3 and 6. If q_j is a generalized coordinate, then the six equations of motion are[9]:

$$\frac{d}{dt}\left(\frac{\partial T}{\partial \dot{q}_j}\right) - \frac{\partial T}{\partial q_j} = Q_j \tag{7}$$

where T is the total kinetic energy of the fluid, t is time, and the Q_j are forces on the fluid associated with the q_j. Note that $Q_j \delta q_j$ always has units of energy, so that when q_j is an angle, Q_j is a moment.

Since it is most convenient to describe the vehicle motion using body axis velocities and forces, it is desirable to write the equations of motion in terms of u, v, w, p, q, r and X, Y, Z, K, M, N (the latter are, respectively, standard notation[8] for the forces and moments on the *vehicle* and are associated with the x, y, z axes). This is most easily done by taking the inertial and body axes to be precisely coincident at the instant in time of interest. Then the Q_j will be the *negative* of the vehicle forces and moments.

The terms on the LHS of equation 7 are expanded as follows:

$$\frac{\partial T}{\partial q_j} = \frac{\partial T}{\partial u}\frac{\partial u}{\partial q_j} + \frac{\partial T}{\partial v}\frac{\partial v}{\partial q_j} + \frac{\partial T}{\partial w}\frac{\partial w}{\partial q_j} + \frac{\partial T}{\partial p}\frac{\partial p}{\partial q_j} + \frac{\partial T}{\partial q}\frac{\partial q}{\partial q_j} + \frac{\partial T}{\partial r}\frac{\partial r}{\partial q_j}. \tag{8}$$

Equations 3 and 6 are used to evaluate the partial derivatives with respect to the q_j at the instant the axes are coincident, when $\dot{x}_0, \dot{y}_0, \dot{z}_0, \dot{\phi}, \dot{\theta}, \dot{\psi} \equiv u, v, w, p, q, r$:

$$\frac{\partial(u,v,w,p,q,r)}{\partial(\dot{x}_0,\dot{y}_0,\dot{z}_0)} = 0; \quad \frac{\partial \mathbf{v}}{\partial(\dot{\phi},\dot{\theta},\dot{\psi})} = \begin{pmatrix} 0, & -w, & v \\ w, & 0, & -u \\ -v, & u, & 0 \end{pmatrix}; \quad \frac{\partial \omega}{\partial(\dot{\phi},\dot{\theta},\dot{\psi})} = \begin{pmatrix} 0, & -, & 0 \\ r, & 0, & 0 \\ -q, & 0, & 0 \end{pmatrix}.$$

The first term of equation 7 becomes:

$$\frac{d}{dt}\left(\frac{\partial T}{\partial \dot{q}_j}\right) = \frac{d}{dt}\left(\frac{\partial T}{\partial u}\frac{\partial u}{\partial \dot{q}_j} + \frac{\partial T}{\partial v}\frac{\partial v}{\partial \dot{q}_j} + \frac{\partial T}{\partial w}\frac{\partial w}{\partial \dot{q}_j} + \frac{\partial T}{\partial p}\frac{\partial p}{\partial \dot{q}_j} + \frac{\partial T}{\partial q}\frac{\partial q}{\partial \dot{q}_j} + \frac{\partial T}{\partial r}\frac{\partial r}{\partial \dot{q}_j}\right) \tag{9}$$

with:

$$\frac{d}{dt}\left(\frac{\partial T}{\partial n}\frac{\partial n}{\partial \dot{q}_j}\right) = \left(\frac{d}{dt}\frac{\partial T}{\partial n}\right)\frac{\partial n}{\partial \dot{q}_j} + \frac{\partial T}{\partial n}\left(\frac{d}{dt}\frac{\partial n}{\partial \dot{q}_j}\right) \tag{10}$$

and, again at the instant of interest, one gets:

$$\frac{\partial(u,v,w)}{\partial(\dot{\phi},\dot{\theta},\dot{\psi})} = \frac{\partial(p,q,r)}{\partial(\dot{x}_0,\dot{y}_0,\dot{z}_0)} = 0; \quad \frac{\partial \mathbf{v}}{\partial(\dot{x}_0,\dot{y}_0,\dot{z}_0)} = \frac{\partial \omega}{\partial(\dot{\phi},\dot{\theta},\dot{\psi})} = \begin{pmatrix} 1,0,0 \\ 0,1,0 \\ 0,0,1 \end{pmatrix}$$

$$\frac{d}{dt}\frac{\partial(u,v,w)}{\partial(\dot{\phi},\dot{\theta},\dot{\psi})} = \frac{d}{dt}\frac{\partial(p,q,r)}{\partial(\dot{x}_0,\dot{y}_0,\dot{z}_0)} = 0$$

$$\frac{d}{dt}\frac{\partial \mathbf{v}}{\partial(\dot{x}_0,\dot{y}_0,\dot{z}_0)} = \begin{pmatrix} 0, & r, & -q \\ -r, & 0, & p \\ q, & -p, & 0 \end{pmatrix}; \quad \frac{d}{dt}\frac{\partial \omega}{\partial(\dot{\phi},\dot{\theta},\dot{\psi})} = \begin{pmatrix} 0, & 0, & -q \\ 0, & 0, & p \\ 0, & -p, & 0 \end{pmatrix}.$$

Thus, the equations of motion given in Lamb are rederived:

$$\begin{aligned}
\frac{d}{dt}\frac{\partial T}{\partial u} - r\frac{\partial T}{\partial v} + q\frac{\partial T}{\partial w} &= -X \\
\frac{d}{dt}\frac{\partial T}{\partial v} - p\frac{\partial T}{\partial w} + r\frac{\partial T}{\partial u} &= -Y \\
\frac{d}{dt}\frac{\partial T}{\partial w} - q\frac{\partial T}{\partial u} + p\frac{\partial T}{\partial v} &= -Z \\
\frac{d}{dt}\frac{\partial T}{\partial p} - w\frac{\partial T}{\partial v} + v\frac{\partial T}{\partial w} - r\frac{\partial T}{\partial q} + q\frac{\partial T}{\partial r} &= -K \\
\frac{d}{dt}\frac{\partial T}{\partial q} - u\frac{\partial T}{\partial w} + w\frac{\partial T}{\partial u} - p\frac{\partial T}{\partial r} + r\frac{\partial T}{\partial p} &= -M \\
\frac{d}{dt}\frac{\partial T}{\partial r} - v\frac{\partial T}{\partial u} + u\frac{\partial T}{\partial v} - q\frac{\partial T}{\partial p} + p\frac{\partial T}{\partial q} &= -N.
\end{aligned} \tag{11}$$

Since the orientation of the inertial axes is arbitrary, these equations are in fact true at any instant in time. An alternative way to write them is:

$$\left[\frac{d}{dt} + \begin{pmatrix} 0 & -r & q & 0 & 0 & 0 \\ r & 0 & -p & 0 & 0 & 0 \\ -q & p & 0 & 0 & 0 & 0 \\ 0 & -w & v & 0 & -r & q \\ w & 0 & -u & r & 0 & -p \\ -v & u & 0 & -q & p & 0 \end{pmatrix}\right] \begin{pmatrix} \partial T/\partial u \\ \partial T/\partial v \\ \partial T/\partial w \\ \partial T/\partial p \\ \partial T/\partial q \\ \partial T/\partial r \end{pmatrix} = - \begin{pmatrix} X \\ Y \\ Z \\ K \\ M \\ N \end{pmatrix}. \tag{12}$$

Equations 11 are linear in T, so that if T is written as a linear combination of the contributions from each body component, then the right and left hand sides of the equations can also be separated into component contributions. This is equivalent to independently applying the equations to separate body components and then summing the resulting component force predictions to give the total force on the body. However, finding the component contributions to T is no easy matter since they must account for the presence of the other components (interference effects).

Equations 11 will be separately applied to each of the many components comprising the vehicle body, with interference effects to be determined later. First, though, the position and orientation of the replacement ellipsoid for each component needs to be specified relative to the vehicle body axes. We begin by considering orientation.

Hydrodynamic considerations will result in one of the ellipsoid's principle axes always being perpendicular to the body x axis, control surface deflections aside. This eliminates one degree of freedom, allowing the ellipsoid to achieve its desired orientation relative to the body axes with only two independent rotations.

Let the x', y', z' axes be the ellipsoid principle axes. Assuming these axes are initially aligned with the body axes, their desired reorientation is achieved by

1) rotating about the x' axis through an angle Φ, and then
2) rotating about the z' axis through an angle Ω.

As before, all rotations are in the positive sense as defined by the Right Hand Rule. This choice of transformation means that the z' axis will always be perpendicular to the body x axis. The matrix $\mathbf{B}$ transforming vectors using a body axes representation to ones using ellipsoidal axes is:

$$\mathbf{B} \equiv \begin{pmatrix} \cos\Omega & \sin\Omega & 0 \\ -\sin\Omega & \cos\Omega & 0 \\ 0 & 0 & 1 \end{pmatrix} \begin{pmatrix} 1 & 0 & 0 \\ 0 & \cos\Phi & \sin\Phi \\ 0 & -\sin\Phi & \cos\Phi \end{pmatrix} = \begin{pmatrix} \cos\Omega & \sin\Omega\cos\Phi & \sin\Omega\sin\Phi \\ -\sin\Omega & \cos\Omega\cos\Phi & \cos\Omega\sin\Phi \\ 0 & -\sin\Phi & \cos\Phi \end{pmatrix}. \tag{13}$$

Besides these rotations, the ellipsoid will have its centroid displaced a distance $\bar{\mathbf{r}} = \bar{x}\mathbf{i} + \bar{y}\mathbf{j} + \bar{z}\mathbf{k}$ relative to the origin of the body axes (using body axis coordinates), so that the velocity of the ellipsoidal axes' origin is:

$$\bar{\mathbf{v}} = \mathbf{v} + \omega \times \bar{\mathbf{r}} = \begin{pmatrix} u + q\bar{z} - r\bar{y} \\ v + r\bar{x} - p\bar{z} \\ w + p\bar{y} - q\bar{x} \end{pmatrix}. \tag{14}$$

In the x', y', z' coordinate system one gets:

$$\mathbf{v}' \equiv \begin{pmatrix} u' \\ v' \\ w' \end{pmatrix} = \mathbf{B}\,\bar{\mathbf{v}} \tag{15}$$

as the translational velocity of the origin. Since the vehicle and its components are undergoing solid body rotation, all of their angular velocities are equal (i.e., $\bar{\omega} = \omega$) and so:

$$\omega' \equiv \begin{pmatrix} p' \\ q' \\ r' \end{pmatrix} = \mathbf{B}\,\omega. \tag{16}$$

Equations 14 through 16 can be summarized in the following matrix equation:

$$\begin{pmatrix} u' \\ v' \\ w' \\ p' \\ q' \\ r' \end{pmatrix} = \mathbf{M} \begin{pmatrix} u \\ v \\ w \\ p \\ q \\ r \end{pmatrix} \tag{17}$$

where:

$$\mathbf{M} \equiv \begin{pmatrix} \mathbf{B} & \mathbf{B}\begin{pmatrix} 0 & \bar{z} & -\bar{y} \\ -\bar{z} & 0 & \bar{x} \\ \bar{y} & -\bar{x} & 0 \end{pmatrix} \\ \mathbf{0} & \mathbf{B} \end{pmatrix}.$$

With the various coordinate systems and their associated variables now established, all that is required are expressions for the kinetic energy of the flow. These are derived in Section 4, where the general expression for the kinetic energy in the flow around an ellipsoid is shown to be:

$$T = \tfrac{1}{2}\rho V \left(t_{11}u'^2 + t_{22}v'^2 + t_{33}w'^2 + t_{44}p'^2 + t_{55}q'^2 + t_{66}r'^2 \right) \tag{18}$$

where ρ is fluid density, V is the volume of the ellipsoid, and the t_{ii} are the inertia coefficients, determined by the ellipsoid's geometry. Using this expression, the column matrix on the LHS of equation 12 becomes:

$$\begin{pmatrix} \partial T/\partial u \\ \partial T/\partial v \\ \partial T/\partial w \\ \partial T/\partial p \\ \partial T/\partial q \\ \partial T/\partial r \end{pmatrix} = \begin{pmatrix} \partial u'/\partial u & \partial v'/\partial u & \dots & \partial r'/\partial u \\ \partial u'/\partial v & \partial v'/\partial v & \dots & \partial r'/\partial v \\ \vdots & \vdots & \ddots & \vdots \\ \partial u'/\partial r & \partial v'/\partial r & \dots & \partial r'/\partial r \end{pmatrix} \begin{pmatrix} \partial T/\partial u' \\ \partial T/\partial v' \\ \partial T/\partial w' \\ \partial T/\partial p' \\ \partial T/\partial q' \\ \partial T/\partial r' \end{pmatrix} = \rho V \, \mathbf{M}^T \mathbf{T} \begin{pmatrix} u' \\ v' \\ w' \\ p' \\ q' \\ r' \end{pmatrix} \tag{19}$$

where:

$$\mathbf{T} \equiv \begin{pmatrix} t_{11} & 0 & 0 & 0 & 0 & 0 \\ 0 & t_{22} & 0 & 0 & 0 & 0 \\ 0 & 0 & t_{33} & 0 & 0 & 0 \\ 0 & 0 & 0 & t_{44} & 0 & 0 \\ 0 & 0 & 0 & 0 & t_{55} & 0 \\ 0 & 0 & 0 & 0 & 0 & t_{66} \end{pmatrix}.$$

(Note that $\mathbf{M}^T \neq \mathbf{M}^{-1}$.) Thus, the equations of motion for one ellipsoidal component of the multi-component body are:

$$\left[\frac{d}{dt} + \begin{pmatrix} 0 & -r & q & 0 & 0 & 0 \\ r & 0 & -p & 0 & 0 & 0 \\ -q & p & 0 & 0 & 0 & 0 \\ 0 & -w & v & 0 & -r & q \\ w & 0 & -u & r & 0 & -p \\ -v & u & 0 & -q & p & 0 \end{pmatrix} \right] \mathbf{M}^T \mathbf{T} \mathbf{M} \begin{pmatrix} u \\ v \\ w \\ p \\ q \\ r \end{pmatrix} = \frac{-1}{\rho V} \begin{pmatrix} X \\ Y \\ Z \\ K \\ M \\ N \end{pmatrix}. \tag{20}$$

Since $\mathbf{T}$ is a diagonal matrix, $\mathbf{M}^T \mathbf{T} \mathbf{M}$ is symmetric. Actually, this equation is true for any arbitrarily shaped body providing $\mathbf{T}$ is allowed to be a fully populated matrix; however, even for this general case, Lamb shows that $\mathbf{T}$ is symmetric and, therefore, that $\mathbf{M}^T \mathbf{T} \mathbf{M}$ is *always* symmetric in an ideal flow.

Multiplying through the differential in equation 20 one gets:

$$\frac{d}{dt} \mathbf{M}^T \mathbf{T} \mathbf{M} \begin{pmatrix} u \\ v \\ w \\ p \\ q \\ r \end{pmatrix} = \mathbf{M}^T \mathbf{T} \mathbf{M} \begin{pmatrix} \dot{u} \\ \dot{v} \\ \dot{w} \\ \dot{p} \\ \dot{q} \\ \dot{r} \end{pmatrix} \tag{21}$$

since $\mathbf{M}^T\,\mathbf{T}\,\mathbf{M}$ is constant for a body with fixed, immovable components. Therefore, it can be identified as the added mass matrix:

$$\begin{pmatrix} X_{\dot{u}} & X_{\dot{v}} & X_{\dot{w}} & X_{\dot{p}} & X_{\dot{q}} & X_{\dot{r}} \\ Y_{\dot{u}} & Y_{\dot{v}} & Y_{\dot{w}} & Y_{\dot{p}} & Y_{\dot{q}} & Y_{\dot{r}} \\ Z_{\dot{u}} & Z_{\dot{v}} & Z_{\dot{w}} & Z_{\dot{p}} & Z_{\dot{q}} & Z_{\dot{r}} \\ K_{\dot{u}} & K_{\dot{v}} & K_{\dot{w}} & K_{\dot{p}} & K_{\dot{q}} & K_{\dot{r}} \\ M_{\dot{u}} & M_{\dot{v}} & M_{\dot{w}} & M_{\dot{p}} & M_{\dot{q}} & M_{\dot{r}} \\ N_{\dot{u}} & N_{\dot{v}} & N_{\dot{w}} & N_{\dot{p}} & N_{\dot{q}} & N_{\dot{r}} \end{pmatrix} \equiv -\rho V\,\mathbf{M}^T\,\mathbf{T}\,\mathbf{M}. \tag{22}$$

Since this matrix is symmetric, $X_{\dot{v}} = Y_{\dot{u}}$, $X_{\dot{w}} = Z_{\dot{u}}$, $Y_{\dot{w}} = Z_{\dot{v}}$, etc. Future calculations may replace a term from below the diagonal of this matrix with its above the diagonal equivalent. Equations 23 give the expressions for the components of the matrix, obtained by evaluating $\mathbf{M}^T\,\mathbf{T}\,\mathbf{M}$.

$$\begin{aligned}
X_{\dot{u}} &= -\rho V\left[\cos^2\Omega\, t_{11} + \sin^2\Omega\, t_{22}\right] \\
X_{\dot{v}} &= -\rho V\left[\cos\Omega\sin\Omega\cos\Phi\,(t_{11} - t_{22})\right] \\
X_{\dot{w}} &= -\rho V\left[\cos\Omega\sin\Omega\sin\Phi\,(t_{11} - t_{22})\right] \\
X_{\dot{p}} &= \bar{y}X_{\dot{w}} - \bar{z}X_{\dot{v}} \\
X_{\dot{q}} &= \bar{z}X_{\dot{u}} - \bar{x}X_{\dot{w}} \\
X_{\dot{r}} &= \bar{x}X_{\dot{v}} - \bar{y}X_{\dot{u}} \\
Y_{\dot{v}} &= -\rho V\left[\sin^2\Omega\cos^2\Phi\, t_{11} + \cos^2\Omega\cos^2\Phi\, t_{22} + \sin^2\Phi\, t_{33}\right] \\
Y_{\dot{w}} &= -\rho V\left[\cos\Phi\sin\Phi\,(\sin^2\Omega\, t_{11} + \cos^2\Omega\, t_{22} - t_{33})\right] \\
Y_{\dot{p}} &= \bar{y}Y_{\dot{w}} - \bar{z}Y_{\dot{v}} \\
Y_{\dot{q}} &= \bar{z}X_{\dot{v}} - \bar{x}Y_{\dot{w}} \\
Y_{\dot{r}} &= \bar{x}Y_{\dot{v}} - \bar{y}X_{\dot{v}} \\
Z_{\dot{w}} &= -\rho V\left[\sin^2\Omega\sin^2\Phi\, t_{11} + \cos^2\Omega\sin^2\Phi\, t_{22} + \cos^2\Phi\, t_{33}\right] \\
Z_{\dot{p}} &= \bar{y}Z_{\dot{w}} - \bar{z}Y_{\dot{w}} \\
Z_{\dot{q}} &= \bar{z}X_{\dot{w}} - \bar{x}Z_{\dot{w}} \\
Z_{\dot{r}} &= \bar{x}Y_{\dot{w}} - \bar{y}X_{\dot{w}} \\
K_{\dot{p}} &= -\rho V\left[\cos^2\Omega\, t_{44} + \sin^2\Omega\, t_{55}\right] + \bar{y}Z_{\dot{p}} - \bar{z}Y_{\dot{p}} \\
K_{\dot{q}} &= -\rho V\left[\cos\Omega\sin\Omega\cos\Phi\,(t_{44} - t_{55})\right] + \bar{y}Z_{\dot{q}} - \bar{z}Y_{\dot{q}} \\
K_{\dot{r}} &= -\rho V\left[\cos\Omega\sin\Omega\sin\Phi\,(t_{44} - t_{55})\right] + \bar{y}Z_{\dot{r}} - \bar{z}Y_{\dot{r}} \\
M_{\dot{q}} &= -\rho V\left[\sin^2\Omega\cos^2\Phi\, t_{44} + \cos^2\Omega\cos^2\Phi\, t_{55} + \sin^2\Phi\, t_{66}\right] + \bar{z}X_{\dot{q}} - \bar{x}Z_{\dot{q}} \\
M_{\dot{r}} &= -\rho V\left[\cos\Phi\sin\Phi\,(\sin^2\Omega\, t_{44} + \cos^2\Omega\, t_{55} - t_{66})\right] + \bar{z}X_{\dot{r}} - \bar{x}Z_{\dot{r}} \\
N_{\dot{r}} &= -\rho V\left[\sin^2\Omega\sin^2\Phi\, t_{44} + \cos^2\Omega\sin^2\Phi\, t_{55} + \cos^2\Phi\, t_{66}\right] + \bar{x}Y_{\dot{r}} - \bar{y}X_{\dot{r}}
\end{aligned} \tag{23}$$

The 'off-diagonal' coefficients mentioned in the Introduction refer to elements of $\mathbf{M}^T\,\mathbf{T}\,\mathbf{M}$.

Equations 23 are only as simple as they are because of the special geometric symmetries of the ellipsoid used to represent a body component. It is obvious that a more fully populated **T** matrix, representing a more general shape, would lead to many additional terms in all of equations 23. In view of this, equations 23 should achieve their greatest accuracy if a body component is replaced with its best representative ellipsoid and the geometry of this replacement ellipsoid is used to calculate the inertia coefficients. This allows errors resulting from 'fitting' the component to be directly monitored and, in fact, to be used in determining the best fit. On the other hand, calculating the t_{ij} for a single component from *different* ellipsoids, or from non-ellipsoidal geometries, in general invalidates equation 18 and will lead to errors of unknown magnitude. These errors, though small relative to the diagonal added mass coefficients, might appreciably affect the smaller off-diagonal terms which contribute to coupling.

Care in fitting the large hull component of a submarine with its replacement ellipsoid is particularly important as, in many cases, the second order effects alluded to in the previous paragraph are roughly the same size as the effects of the appendages. Fitting replacement ellipsoids to appendages is obviously less important.

Equation 21 is the unsteady part of the equations of motion. Using the notation defined in equation 22, and upon breaking equation 20 into its component parts, one obtains equations 24 (on the next page), which are the complete set of expressions[8] for the fluid forces and moments on a vehicle (or one of its components) moving through an ideal fluid.

In addition to the added mass contributions to the forces ($X_{\dot{u}}\dot{u}$, $X_{\dot{v}}\dot{v}$, ..., $N_{\dot{r}}\dot{r}$), which are only important during unsteady maneuvers, equations 24 also give the ideal forces associated with steady state motions (the reader may recognize the M equation term $(X_{\dot{u}} - Z_{\dot{w}})uw$, for example, as a 'Munk moment'[10]). However, many of these ideal steady state terms are known to be strongly subject to viscous effects and, where possible, should be replaced with estimates based on experiment.

For the complete body, equations 24 can be simplified if the vehicle is symmetric about a longitudinal vertical plane, as most submarines are. Then, 9 of the 15 'above the diagonal' summed added mass terms are zero, namely:

$$X_{\dot{v}}, X_{\dot{p}}, X_{\dot{r}}, Y_{\dot{w}}, Y_{\dot{q}}, Z_{\dot{p}}, Z_{\dot{r}}, K_{\dot{q}}, M_{\dot{r}} .$$

Of course, their 'below the diagonal' counterparts are also zero and, in fact, it is by considering some of these latter terms that one can most easily see that a term must be zero. Thus, for conventional submarine shapes, equations 24 reduce to equations 25.

$$
\begin{aligned}
X &= X_{\dot u}\dot u + X_{\dot v}(\dot v - ur) + X_{\dot w}(\dot w + uq) + X_{\dot p}\dot p + X_{\dot q}\dot q + X_{\dot r}\dot r \\
&\quad - Y_{\dot v}vr + Y_{\dot w}(vq - wr) - Y_{\dot p}rp + (Z_{\dot r} - Y_{\dot q})qr - Y_{\dot r}r^2 + Z_{\dot w}wq + Z_{\dot q}q^2 + Z_{\dot p}pq \\
Y &= X_{\dot v}(\dot u + vr) + Y_{\dot v}\dot v + Y_{\dot w}(\dot w - vp) + Y_{\dot p}\dot p + Y_{\dot q}\dot q + Y_{\dot r}\dot r \\
&\quad + X_{\dot u}ur + X_{\dot w}(wr - up) + (X_{\dot p} - Z_{\dot r})rp + X_{\dot q}qr + X_{\dot r}r^2 - Z_{\dot w}wp - Z_{\dot p}p^2 - Z_{\dot q}pq \\
Z &= X_{\dot w}(\dot u - wq) + Y_{\dot w}(\dot v + wp) + Z_{\dot w}\dot w + Z_{\dot p}\dot p + Z_{\dot q}\dot q + Z_{\dot r}\dot r \\
&\quad - X_{\dot u}uq + X_{\dot v}(up - vq) + (Y_{\dot q} - X_{\dot p})pq - X_{\dot q}q^2 - X_{\dot r}qr + Y_{\dot v}vp + Y_{\dot p}p^2 + Y_{\dot r}rp \\
K &= X_{\dot p}\dot u + Y_{\dot p}(\dot v - wp) + Z_{\dot p}(\dot w + vp) + K_{\dot p}\dot p + K_{\dot q}(\dot q - rp) + K_{\dot r}(\dot r + pq) \\
&\quad - X_{\dot v}uw + X_{\dot w}uv - X_{\dot q}ur + X_{\dot r}uq + (Z_{\dot w} - Y_{\dot v})vw + Y_{\dot w}(v^2 - w^2) \\
&\quad - (Y_{\dot q} - Z_{\dot r})(vr + wq) + (Y_{\dot r} + Z_{\dot q})(vq - wr) - (M_{\dot q} - N_{\dot r})qr + M_{\dot r}(q^2 - r^2) \\
M &= X_{\dot q}(\dot u + wq) + Y_{\dot q}\dot v + Z_{\dot q}(\dot w - uq) + K_{\dot q}(\dot p + qr) + M_{\dot q}\dot q + M_{\dot r}(\dot r - pq) \\
&\quad + (X_{\dot u} - Z_{\dot w})uw + X_{\dot v}vw + X_{\dot w}(w^2 - u^2) + (X_{\dot p} - Z_{\dot r})(wp + ur) \\
&\quad - (X_{\dot r} + Z_{\dot p})(up - wr) - Y_{\dot w}uv + Y_{\dot p}vr - Y_{\dot r}vp + (K_{\dot p} - N_{\dot r})pr - K_{\dot r}(p^2 - r^2) \\
N &= X_{\dot r}(\dot u - vr) + Y_{\dot r}(\dot v + ur) + Z_{\dot r}\dot w + K_{\dot r}(\dot p - qr) + M_{\dot r}(\dot q + pr) + N_{\dot r}\dot r \\
&\quad - (X_{\dot u} - Y_{\dot v})uv + X_{\dot v}(u^2 - v^2) - X_{\dot w}vw - (X_{\dot p} - Y_{\dot q})(uq + vp) \\
&\quad + (X_{\dot q} + Y_{\dot p})(up - vq) + Y_{\dot w}uw - Z_{\dot p}wq + Z_{\dot q}wp - (K_{\dot p} - M_{\dot q})pq + K_{\dot q}(p^2 - q^2)
\end{aligned}
\tag{24}
$$

$$
\begin{aligned}
X &= X_{\dot u}\dot u + X_{\dot w}(\dot w + uq) + X_{\dot q}\dot q - Y_{\dot v}vr - Y_{\dot p}rp - Y_{\dot r}r^2 + Z_{\dot w}wq + Z_{\dot q}q^2 \\
Y &= Y_{\dot v}\dot v + Y_{\dot p}\dot p + Y_{\dot r}\dot r + X_{\dot u}ur + X_{\dot w}(wr - up) + X_{\dot q}qr - Z_{\dot w}wp - Z_{\dot q}pq \\
Z &= X_{\dot w}(\dot u - wq) + Z_{\dot w}\dot w + Z_{\dot q}\dot q - X_{\dot u}uq - X_{\dot q}q^2 + Y_{\dot v}vp + Y_{\dot p}p^2 + Y_{\dot r}rp \\
K &= Y_{\dot p}(\dot v - wp) + K_{\dot p}\dot p + K_{\dot r}(\dot r + pq) + X_{\dot w}uv - X_{\dot q}ur \\
&\quad + (Z_{\dot w} - Y_{\dot v})vw + (Y_{\dot r} + Z_{\dot q})(vq - wr) - (M_{\dot q} - N_{\dot r})qr \\
M &= X_{\dot q}(\dot u + wq) + Z_{\dot q}(\dot w - uq) + M_{\dot q}\dot q + (X_{\dot u} - Z_{\dot w})uw \\
&\quad + X_{\dot w}(w^2 - u^2) + Y_{\dot p}vr - Y_{\dot r}vp + (K_{\dot p} - N_{\dot r})pr - K_{\dot r}(p^2 - r^2) \\
N &= Y_{\dot r}(\dot v + ur) + K_{\dot r}(\dot p - qr) + N_{\dot r}\dot r - (X_{\dot u} - Y_{\dot v})uv - X_{\dot w}vw \\
&\quad + (X_{\dot q} + Y_{\dot p})(up - vq) + Z_{\dot q}wp - (K_{\dot p} - M_{\dot q})pq
\end{aligned}
\tag{25}
$$

3 Interference Effects: Primary and Secondary Components

The equations of motion, as summarized in equation 20, apply only to an isolated body. Thus, equations 23 do not account for any modification of the flow about the ellipsoid due to the presence of another body. In this section, these interference effects will be modelled approximately by superimposing a uniform velocity over a relatively small ellipsoid which finds itself in the presence of a larger one; this *interference velocity* will be the velocity field around the large ellipsoid evaluated at the location of the centroid of the smaller one, without the smaller ellipsoid being present.

Formally, a body component will be assigned one of two possible orders: either *primary* or *secondary*. In general, one would call the hull a primary component and a hull appendage a secondary component. Primary component added masses are not corrected for interference effects. Secondary component added masses are only corrected for the presence of the primary component; all other components are ignored.

Thus, equations 20 and 23 are correct for all primary body components. For secondary components, a modification must be made in the development of equation 20, at the level of equation 17. In this latter equation, the interference velocity must be subtracted from u, v, w to give the effective velocity of the secondary ellipsoid through the fluid. There is no correction to p, q, r since the potential flow about the primary ellipsoid can have no rotation in the field; however, as primary component body angular velocities, p, q, r will certainly contribute to the corrections applied to u, v, w.

Now, denote the interference velocity due to a primary component moving with velocity u as $\bar{u}_u u\mathbf{i} + \bar{v}_u u\mathbf{j} + \bar{w}_u u\mathbf{k}$, velocity v as $\bar{u}_v v\mathbf{i} + \bar{v}_v v\mathbf{j} + \bar{w}_v v\mathbf{k}$, ..., and angular velocity r as $\bar{u}_r r\mathbf{i} + \bar{v}_r r\mathbf{j} + \bar{w}_r r\mathbf{k}$. Here, the bar over a variable indicates the velocity is that at the location of the centroid of the secondary ellipsoid. These variables are dimensionless if their subscripts are u, v, or w, they have dimensions of length if their subscripts are p, q, or r. The velocity vector on the right hand side of equation 17 can now be rewritten:

$$\begin{pmatrix} u \\ v \\ w \\ p \\ q \\ r \end{pmatrix} \longrightarrow \begin{pmatrix} 1-\bar{u}_u & -\bar{u}_v & -\bar{u}_w & -\bar{u}_p & -\bar{u}_q & -\bar{u}_r \\ -\bar{v}_u & 1-\bar{v}_v & -\bar{v}_w & -\bar{v}_p & -\bar{v}_q & -\bar{v}_r \\ -\bar{w}_u & -\bar{w}_v & 1-\bar{w}_w & -\bar{w}_p & -\bar{w}_q & -\bar{w}_r \\ 0 & 0 & 0 & 1 & 0 & 0 \\ 0 & 0 & 0 & 0 & 1 & 0 \\ 0 & 0 & 0 & 0 & 0 & 1 \end{pmatrix} \begin{pmatrix} u \\ v \\ w \\ p \\ q \\ r \end{pmatrix} \equiv \mathbf{F} \begin{pmatrix} u \\ v \\ w \\ p \\ q \\ r \end{pmatrix} \tag{26}$$

where $\mathbf{F}$ is the *interference matrix*. This multiplication by $\mathbf{F}$ is equivalent to subtracting the interference velocities from $\bar{\mathbf{v}}$, equation 14. Equation 17 becomes:

$$\begin{pmatrix} u' \\ v' \\ w' \\ p' \\ q' \\ r' \end{pmatrix} = \mathbf{MF} \begin{pmatrix} u \\ v \\ w \\ p \\ q \\ r \end{pmatrix}. \tag{27}$$

Equation 20 will then be applicable to secondary components if $\mathbf{M}^T\mathbf{TM}$ is replaced with $\mathbf{F}^T\mathbf{M}^T\mathbf{TMF}$, which is the new added mass matrix.

If, for a secondary component, the elements of the matrix $-\rho V\,\mathbf{M}^T\,\mathbf{T}\,\mathbf{M}$ are denoted $X^0_{\dot{u}}$, $X^0_{\dot{v}}$, ..., $N^0_{\dot{r}}$ (the values of these elements are given by equations 23 and they would be the true added masses if there were no interference), then the secondary component added masses are:

$$\begin{aligned}
X_{\dot{u}} &= (1-\bar{u}_u)\left[X^0_{\dot{u}}(1-\bar{u}_u) - X^0_{\dot{v}}\bar{v}_u - X^0_{\dot{w}}\bar{w}_u\right] \\
&\quad - \bar{v}_u\left[X^0_{\dot{v}}(1-\bar{u}_u) - Y^0_{\dot{v}}\bar{v}_u - Y^0_{\dot{w}}\bar{w}_u\right] - \bar{w}_u\left[X^0_{\dot{w}}(1-\bar{u}_u) - Y^0_{\dot{w}}\bar{v}_u - Z^0_{\dot{w}}\bar{w}_u\right] \\
X_{\dot{v}} &= (1-\bar{u}_u)\left[-X^0_{\dot{u}}\bar{u}_v + X^0_{\dot{v}}(1-\bar{v}_v) - X^0_{\dot{w}}\bar{w}_v\right] \\
&\quad - \bar{v}_u\left[-X^0_{\dot{v}}\bar{u}_v + Y^0_{\dot{v}}(1-\bar{v}_v) - Y^0_{\dot{w}}\bar{w}_v\right] - \bar{w}_u\left[-X^0_{\dot{w}}\bar{u}_v + Y^0_{\dot{w}}(1-\bar{v}_v) - Z^0_{\dot{w}}\bar{w}_v\right] \qquad (28) \\
&\vdots \\
N_{\dot{r}} &= N^0_{\dot{r}} - \bar{u}_r\left[2X^0_{\dot{r}} - X^0_{\dot{u}}\bar{u}_r - X^0_{\dot{v}}\bar{v}_r - X^0_{\dot{w}}\bar{w}_r\right] \\
&\quad - \bar{v}_r\left[2Y^0_{\dot{r}} - X^0_{\dot{v}}\bar{u}_r - Y^0_{\dot{v}}\bar{v}_r - Y^0_{\dot{w}}\bar{w}_r\right] - \bar{w}_r\left[2Z^0_{\dot{r}} - X^0_{\dot{w}}\bar{u}_r - Y^0_{\dot{w}}\bar{v}_r - Z^0_{\dot{w}}\bar{w}_r\right]
\end{aligned}$$

(The complete set of added masses are easily obtained by matrix multiplication.) Note that the corrections for interference effects are proportional to second order products in the interference velocities. This is because added mass is a measure of fluid kinetic energy, which varies as the square of the fluid velocity. Thus, these corrections are potentially very important.

As with the elements of the matrix $\mathbf{M}^T\,\mathbf{T}\,\mathbf{M}$, the elements of the inteference matrix $\mathbf{F}$ are purely a function of vehicle geometry, as will be shown in following sections.

It is noteworthy that interference effects change some of the relationships between the added mass coefficients presented in equations 23. Consider the simple example of an axisymmetric hull ellipsoid with a sail positioned directly over its center of buoyancy. For roll and sway motions, write the fluid kinetic energy due to the sail as $T = \frac{1}{2}\rho V(t_{22}v'^2 + t_{44}p'^2)$ with $p' = p$ and $v' = v - \bar{z}p - \bar{v}_v v$, the last term in the latter equation being the interference velocity at the sail due to the presence of the hull; $\bar{z}$ locates the sail's centroid. (For this example, it is convenient to take the sail's y' axis to be parallel to the body y axis, unlike the general notation presented in Section 8.) If $\kappa \equiv 1 - \bar{v}_v$, $v' = \kappa v - \bar{z}p$; $\bar{v}_v$ will be negative, so $\kappa > 1$. Then, the time dependent parts of the second and fourth of equations 1 result in:

$$\begin{gathered}
Y_{\dot{v}} = \kappa^2 Y^0_{\dot{v}}; \quad Y_{\dot{p}}, K_{\dot{v}} = -\kappa\bar{z}Y^0_{\dot{v}}; \\
K_{\dot{p}} = K^0_{\dot{p}} = -\rho V t_{44} + \bar{z}^2 Y^0_{\dot{v}}
\end{gathered} \qquad (29)$$

As expected, $Y_{\dot{v}}$ is proportional to κ^2, and $K_{\dot{p}}$ is unaffected by interference effects since the axisymmetric hull can rotate without generating an interference velocity. However, note that $K_{\dot{v}} \neq -\bar{z}Y_{\dot{v}}$ and that the '$Y_{\dot{p}}$' contribution to $K_{\dot{p}}$ is not $-\bar{z}Y_{\dot{p}}$ as in equations 23. Symmetry of the added mass matrix requires $Y_{\dot{p}} = K_{\dot{v}}$, and this prevents the usual inter-relationships among the coefficients from occuring.

In the above example, κ will be less than 2 (a value corresponding to an infinitely small sail with its centroid located right on the hull surface). For an asymmetric hull, with its major transverse axis aligned with the sail, κ will be larger than it would be for an axisymmetric hull.

4 The Kinetic Energy in the Ideal Flow Around an Ellipsoid

In Section 2, expressions for the added mass of an ellipsoid in an ideal flow are obtained in terms of the flow's kinetic energy. In this section, expressions for the kinetic energy are presented. Their complete derivation is presented in Lamb[2], beginning in article 111. This derivation is most conveniently carried out using confocal ellipsoidal coordinates. Both Lamb and Whittaker and Watson[11], chapter 23, present the necessary details for use of this coordinate system.

The kinetic energy T of the flow can be obtained if the velocity potential φ is known in the inertial reference frame of Section 2. $\varphi(x_0, y_0, z_0)$ must satisfy Laplace's equation $\nabla^2\varphi = 0$ subject to boundary conditions at infinity and the ellipsoid surface. The flow velocity at any point is then $\mathbf{v}_0 = -\nabla\varphi$, and the kinetic energy of the flow will be given by:

$$2T = -\rho \iint \varphi \frac{\partial \varphi}{\partial n}\, dS\,. \tag{30}$$

The integration is over the surface of the ellipsoid; n is the direction normal to the surface into the fluid.

In the inertial reference frame, the equation for an ellipsoid with principal axes of length $2a$, $2b$, and $2c$ is:

$$\frac{x_0^2}{a^2} + \frac{y_0^2}{b^2} + \frac{z_0^2}{c^2} - 1 = 0\,. \tag{31}$$

The equation of any confocal quadric to this ellipsoid is:

$$\frac{x_0^2}{a^2+\theta} + \frac{y_0^2}{b^2+\theta} + \frac{z_0^2}{c^2+\theta} - 1 = 0 \tag{32}$$

where θ is the *parameter* of the quadric. This last expression can be solved for θ for any point (x_0, y_0, z_0). Since the solution is that of a cubic polynomial in θ, there are, in general, three quadrics passing through (x_0, y_0, z_0). The confocal ellipsoidal coordinates, denoted λ, μ, ν, are the three roots of this cubic. If ξ, σ, τ are the largest, second largest, and smallest, respectively, of a, b, c, then $-\xi^2 < \nu < -\sigma^2 < \mu < -\tau^2 < \lambda < \infty$. The quadric surfaces $\lambda, \mu, \nu =$ constant are ellipsoids, hyperboloids of one sheet, and hyperboloids of two sheets respectively. These surfaces are always mutually orthogonal.

Consider, now, the potential flow around an ellipsoid translating through a stationary fluid with velocity u in the direction of one of its principal axes. At the instant in time of interest, the centroid of the ellipsoid is precisely coincident with the origin of the inertial x_0, y_0, z_0 axes such that its surface is given by equation 31 and u is directed along the the x_0 axis. Lamb shows that a solution to Laplace's equation of the form:

$$\varphi_1 = x_0 \chi_1(\lambda) u \tag{33}$$

is capable of satisfying the boundary conditions for this instant in time. He gets:

$$\chi_1(\lambda) = \frac{abc}{2-\alpha_0} \int_\lambda^\infty \frac{d\lambda}{(a^2+\lambda)\Delta} \tag{34}$$

where:

$$\alpha_0 \equiv abc \int_0^\infty \frac{d\lambda}{(a^2+\lambda)\Delta}\,, \qquad \Delta \equiv \sqrt{(a^2+\lambda)(b^2+\lambda)(c^2+\lambda)}\,. \tag{35}$$

A simple cyclic permutation of variables:

$$a \rightarrow b \rightarrow c \quad \text{and} \quad x_0 \rightarrow y_0 \rightarrow z_0 \qquad \text{as} \qquad u \rightarrow v \rightarrow w$$

in equations 33 through 35 gives the expressions for φ_2 and φ_3, for translation in the directions of the other two principal axes:

$$\varphi_2 = y_0 \chi_2(\lambda) v, \quad \chi_2(\lambda) = \frac{abc}{2 - \beta_0} \int_\lambda^\infty \frac{d\lambda}{(b^2 + \lambda)\Delta} \tag{36}$$

$$\varphi_3 = z_0 \chi_3(\lambda) w, \quad \chi_3(\lambda) = \frac{abc}{2 - \gamma_0} \int_\lambda^\infty \frac{d\lambda}{(c^2 + \lambda)\Delta} \tag{37}$$

where:

$$\beta_0 \equiv abc \int_0^\infty \frac{d\lambda}{(b^2 + \lambda)\Delta}, \quad \gamma_0 \equiv abc \int_0^\infty \frac{d\lambda}{(c^2 + \lambda)\Delta}. \tag{38}$$

a, b, and c, then, are the semi-axis lengths of the ellipsoid principal axes parallel to the directions of u, v, and w respectively.

Consider, also, an ellipsoid rotating in a stationary ideal fluid with angular velocity p about one of its principal axes. At the instant in time of interest, its surface is given by equation 31 and the aforementioned principal axis coincides with the x_0 axis. Again, Lamb shows that:

$$\varphi_4 = y_0 z_0 \chi_4(\lambda) p \tag{39}$$

satisfies these boundary conditions, where:

$$\chi_4(\lambda) = \frac{abc(b^2 - c^2)^2}{2(b^2 - c^2) + (b^2 + c^2)(\beta_0 - \gamma_0)} \int_\lambda^\infty \frac{d\lambda}{(b^2 + \lambda)(c^2 + \lambda)\Delta}. \tag{40}$$

A cyclic permutation in these last two equations of a, b, c and x_0, y_0, z_0 with p, q, r gives φ_5 and φ_6, the potentials for rotation about the y_0 and z_0 axes with velocities q and r, respectively.

Thus, at the instant in time of interest, the linearity of Laplace's equation allows the potential flow around an ellipsoid moving in 6 degrees of freedom to be written as:

$$\varphi = \varphi_1 + \varphi_2 + \varphi_3 + \varphi_4 + \varphi_5 + \varphi_6. \tag{41}$$

Equation 30 then gives the kinetic energy in the flow:

$$2T = -\rho \sum_{i=1}^{6} \sum_{j=1}^{6} \iint \varphi_i \frac{\partial \varphi_j}{\partial n} \, dS.$$

Because of the geometrical symmetry of an ellipsoid, only the $i = j$ terms of this summation are nonzero. One gets:

$$T = \tfrac{1}{2} \rho V \left(t_{11} u^2 + t_{22} v^2 + t_{33} w^2 + t_{44} p^2 + t_{55} q^2 + t_{66} r^2 \right) \tag{42}$$

where $V = \frac{4}{3}\pi abc$ is the volume of the ellipsoid and the t_{ii} are the inertia coefficients:

$$t_{11} = \frac{\alpha_0}{2-\alpha_0}, \quad t_{22} = \frac{\beta_0}{2-\beta_0}, \quad t_{33} = \frac{\gamma_0}{2-\gamma_0},$$

$$t_{44} = \frac{1}{5}\frac{(b^2-c^2)^2(\gamma_0-\beta_0)}{2(b^2-c^2)+(b^2+c^2)(\beta_0-\gamma_0)}, \quad t_{55} = \frac{1}{5}\frac{(c^2-a^2)^2(\alpha_0-\gamma_0)}{2(c^2-a^2)+(c^2+a^2)(\gamma_0-\alpha_0)}, \quad (43)$$

$$t_{66} = \frac{1}{5}\frac{(a^2-b^2)^2(\beta_0-\alpha_0)}{2(a^2-b^2)+(a^2+b^2)(\alpha_0-\beta_0)}.$$

Although equation 42 was derived for one instant in time, when the ellipsoid is aligned with a purely arbitrary set of inertial axes, the equation applies generally since at any other time there will be another set of inertial axes for which an identical derivation could be performed. Note that, although the notation is different, equation 42 is identical to equation 18 (in each case the velocities are relative to the ellipsoid principal axes).

The integrals in equations 34 through 38 and equation 40 are, in general, elliptic integrals. Their general solutions are presented in Section 6, along with simplifications that can be made in special cases.

5 The Interference Velocity Field Around a Primary Ellipsoid

The elements of the interference matrix of equation 27 can be found by differentiating the velocity potentials of the previous section. At the instant in time of interest, the velocity at any point in the flow field around a primary ellipsoid is $\mathbf{v} = \mathbf{v}_0 = -\nabla\varphi$ (cf, eq. 2), where φ is given by equation 41 and the ellipsoid's boundary by equation 31. The differentiation is aided by the following expression which follows from relationships between the ellipsoidal and cartesian coordinates[3]:

$$\nabla\chi(\lambda) = \frac{h_1^2}{2}\frac{d\chi}{d\lambda}\left(\frac{x_0}{a^2+\lambda}\mathbf{i} + \frac{y_0}{b^2+\lambda}\mathbf{j} + \frac{z_0}{c^2+\lambda}\mathbf{k}\right). \quad (44)$$

Here, $\chi(\lambda)$ is any function of λ; (x_0, y_0, z_0) is any point in the flow field; h_1 is a scale factor relating lengths between the ellipsoidal and cartesian coordinate systems:

$$h_1^2 = 4\left(\frac{x_0^2}{(a^2+\lambda)^2} + \frac{y_0^2}{(b^2+\lambda)^2} + \frac{z_0^2}{(c^2+\lambda)^2}\right)^{-1}. \quad (45)$$

If $\chi(\lambda)$ is identified with the $\chi_i(\lambda)$ defined in the previous section, then equation 44 can be rewritten as:

$$\nabla\chi_i(\lambda) = -\frac{h_1^2 abc}{2\Delta}\left(\frac{x_0}{a^2+\lambda}\mathbf{i} + \frac{y_0}{b^2+\lambda}\mathbf{j} + \frac{z_0}{c^2+\lambda}\mathbf{k}\right)R_i \quad (46)$$

with:

$$R_1 = \frac{1}{(2-\alpha_0)(a^2+\lambda)}, \quad R_4 = \frac{(b^2-c^2)^2}{[2(b^2-c^2)+(b^2+c^2)(\beta_0-\gamma_0)](b^2+\lambda)(c^2+\lambda)}. \quad (47)$$

R_2, R_3 and R_5, R_6 are obtained by cyclically permutating the variables in R_1 and R_4, respectively.

Now, if (x_0, y_0, z_0) is the location of the centroid of a secondary ellipsoid (coincident with (x, y, z) at the instant in time of interest), and if these coordinates determine $\bar{\lambda}$ through a solution of equation 32, then the interference velocities for the secondary ellipsoid are:

$$\begin{aligned}
-\nabla\varphi_1/u &= u_u\mathbf{i} + v_u\mathbf{j} + w_u\mathbf{k} = -\chi_1(\bar{\lambda})\mathbf{i} - x_0\nabla\chi_1(\bar{\lambda}) \\
-\nabla\varphi_2/v &= u_v\mathbf{i} + v_v\mathbf{j} + w_v\mathbf{k} = -\chi_2(\bar{\lambda})\mathbf{j} - y_0\nabla\chi_2(\bar{\lambda}) \\
-\nabla\varphi_3/w &= u_w\mathbf{i} + v_w\mathbf{j} + w_w\mathbf{k} = -\chi_3(\bar{\lambda})\mathbf{k} - z_0\nabla\chi_3(\bar{\lambda}) \\
-\nabla\varphi_4/p &= u_p\mathbf{i} + v_p\mathbf{j} + w_p\mathbf{k} = -x_0\chi_4(\bar{\lambda})\mathbf{j} - y_0\chi_4(\bar{\lambda})\mathbf{k} - y_0z_0\nabla\chi_4(\bar{\lambda}) \\
-\nabla\varphi_5/q &= u_q\mathbf{i} + v_q\mathbf{j} + w_q\mathbf{k} = -x_0\chi_5(\bar{\lambda})\mathbf{i} - z_0\chi_5(\bar{\lambda})\mathbf{k} - z_0x_0\nabla\chi_5(\bar{\lambda}) \\
-\nabla\varphi_6/r &= u_r\mathbf{i} + v_r\mathbf{j} + w_r\mathbf{k} = -y_0\chi_6(\bar{\lambda})\mathbf{i} - x_0\chi_6(\bar{\lambda})\mathbf{j} - x_0y_0\nabla\chi_6(\bar{\lambda}).
\end{aligned} \tag{48}$$

The $\nabla\chi_i(\bar{\lambda})$ on the right hand sides of these equations are easily evaluated in terms of elementary functions of a, b, c, x_0, y_0, z_0, as per equation 46. However, the $\chi_i(\bar{\lambda})$ are elliptic integrals. These constants are evaluated in the next section. Elliptic function theory must be used if the primary component is asymmetric; this is not a difficult problem if the routines necessary for calculating the inertia coefficients for this geometry are already in place. An alternative approach would be to use the 2-D potential flow field around an ellipse to estimate the transverse components of the interference velocities, which are really the only ones of interest. The advantage of the 3-D calculation is that end effects are properly modelled, for example, in the region of a submarine's tail. As will be seen, if the primary component is axisymmetric, then the general 3-D calculations can be carried out using only elementary functions.

6 Evaluating the Inertia Coefficients and Interference Velocities

The inertia coefficients (equations 43) are functions of a, b, and c through the elliptic integrals α_0, β_0, and γ_0 (equations 35 and 38). These same integrals, but with different limits, need to be evaluated when calculating the $\chi_i(\bar{\lambda})$ which are present in the expressions for the interference velocities. In evaluating the integrals, extensive use is made of the theory of elliptic functions. A brief introduction to these functions is given in Appendix A.

There are basically three integrals to be solved:

$$I_1 = \xi\sigma r\int_\lambda^\infty \frac{d\lambda}{(\xi^2+\lambda)\Delta}, \quad I_2 = \xi\sigma r\int_\lambda^\infty \frac{d\lambda}{(\sigma^2+\lambda)\Delta}, \quad I_3 = \xi\sigma r\int_\lambda^\infty \frac{d\lambda}{(r^2+\lambda)\Delta} \tag{49}$$

with:

$$\Delta \equiv \sqrt{(\xi^2+\lambda)(\sigma^2+\lambda)(r^2+\lambda)}.$$

Here, ξ, σ, r are the largest, second largest, and smallest, respectively, of the semi-axes a, b, c of the ellipsoid principal axes. Before obtaining the general solutions to these integrals, some special cases are examined.

A sphere: $\xi = \sigma = r$

In this case:

$$I_1 = I_2 = I_3 = \xi^3 \int_\lambda^\infty \frac{d\lambda}{(\xi^2+\lambda)^{5/2}} = \frac{2}{3}\frac{\xi^3}{(\xi^2+\lambda)^{3/2}}. \tag{50}$$

Thus, $\alpha_0 = \beta_0 = \gamma_0 = 2/3$ **so that** $t_{11} = t_{22} = t_{33} = 1/2$ **and** $t_{44} = t_{55} = t_{66} = 0$.

A prolate spheroid: $\sigma = r$

In this case:

$$\begin{aligned} I_1 &= \xi\sigma^2 \int_\lambda^\infty \frac{d\lambda}{(\sigma^2+\lambda)(\xi^2+\lambda)^{3/2}} \\ &= \frac{-\sigma^2}{\xi^2-\sigma^2}\left(\frac{2\xi}{\sqrt{\xi^2+\lambda}} + \frac{\xi}{\sqrt{\xi^2-\sigma^2}}\ln\frac{\sqrt{\xi^2+\lambda}-\sqrt{\xi^2-\sigma^2}}{\sqrt{\xi^2+\lambda}+\sqrt{\xi^2-\sigma^2}}\right). \end{aligned} \tag{51}$$

Using the eccentricity $e \equiv \sqrt{\xi^2-\sigma^2}/\xi$, **one can duplicate the expression given by Lamb[2] for** $\lambda = 0$:

$$I_1 = \frac{2(1-e^2)}{e^3}\left(\frac{1}{2}\ln\frac{1+e}{1-e} - e\right).$$

Also:

$$I_2 = I_3 = \xi\sigma^2 \int_\lambda^\infty \frac{d\lambda}{(\sigma^2+\lambda)^2\sqrt{\xi^2+\lambda}} = \frac{\xi\sigma^2}{(\sigma^2+\lambda)\sqrt{\xi^2+\lambda}} - \frac{1}{2}I_1. \tag{52}$$

An oblate spheroid: $\xi = \sigma$

Here:

$$\begin{aligned} I_3 = \xi^2 r \int_\lambda^\infty \frac{d\lambda}{(\xi^2+\lambda)(r^2+\lambda)^{3/2}} &= \frac{2\xi^2}{\xi^2-r^2}\left(\frac{r}{\sqrt{r^2+\lambda}} - \frac{r}{\sqrt{\xi^2-r^2}}\sin^{-1}\sqrt{\frac{\xi^2-r^2}{\xi^2+\lambda}}\right) \\ &\sim \frac{2}{e^2}\left(1 - \frac{\sqrt{1-e^2}}{e}\sin^{-1}e\right) \qquad \text{as } \lambda \to 0, \end{aligned} \tag{53}$$

where $e \equiv \sqrt{\xi^2-r^2}/\xi$. **Also:**

$$I_1 = I_2 = \xi^2 r \int_\lambda^\infty \frac{d\lambda}{(\xi^2+\lambda)^2\sqrt{r^2+\lambda}} = \frac{\xi^2 r}{(\xi^2+\lambda)\sqrt{r^2+\lambda}} - \frac{1}{2}I_3. \tag{54}$$

The only other special condition that needs to be considered is when $r = 0$, which is of practical importance if one wishes to model flat plate control surfaces (as is sometimes done). Unfortunately, this apparent simplification complicates matters (in ellipsoidal coordinates, at least). Not only must elliptic functions still be evaluated, in general, but some of the inertia coefficients of equations 43 become singular — a condition that can be remedied by considering the expansion of the t_{ij} for small r and multiplying the result by V. This process will be presented following the general solutions of equations 49.

The general case

It is convenient to make the following variable transformation in equations 49, as per Munk[12] (it is conventional to use the variable u as argument in the Jacobian elliptic functions; u has nothing to do with the velocity defined in previous sections):

$$\lambda = \frac{\xi^2 - \tau^2}{\mathrm{sn}^2 u} - \xi^2 \tag{55}$$

where, as is usual, the Jacobian elliptic function $\mathrm{sn}(u,k)$ is written as $\mathrm{sn}\, u$. k is the modulus of the elliptic function. If:

$$k^2 \equiv \frac{\xi^2 - \sigma^2}{\xi^2 - \tau^2} \qquad \text{so that} \qquad 0 < k < 1\,, \tag{56}$$

then:

$$I_1 = C\int_0^u \mathrm{sn}^2 u\, du\,, \quad I_2 = C\int_0^u \frac{\mathrm{sn}^2 u}{\mathrm{dn}^2 u}\, du\,, \quad I_3 = C\int_0^u \frac{\mathrm{sn}^2 u}{\mathrm{cn}^2 u}\, du \tag{57}$$

where:

$$C \equiv \frac{2\xi\sigma\tau}{(\xi^2 - \tau^2)^{3/2}}\,.$$

Rearranging equation 55 and using equations A2, one gets:

$$\mathrm{sn}^2 u = \frac{\xi^2 - \tau^2}{\xi^2 + \lambda}\,, \quad \mathrm{cn}^2 u = \frac{\tau^2 + \lambda}{\xi^2 + \lambda}\,, \quad \mathrm{dn}^2 u = \frac{\sigma^2 + \lambda}{\xi^2 + \lambda}\,. \tag{58}$$

It is convenient to rewrite the integrals of equations 57 in terms of incomplete elliptic integrals of the first and second kinds, u and $E(u)$ respectively. Thus:

$$\begin{aligned}
&\int_0^u \mathrm{sn}^2 u\, du = \frac{1}{k^2}\left[u - E(u)\right] \sim \frac{1}{k^2}\left[u_0 - E(u_0)\right] \quad \text{as } \lambda \to 0,\ u \to u_0;\\
&\int_0^u \frac{\mathrm{sn}^2 u}{\mathrm{dn}^2 u}\, du = \frac{-\,\mathrm{sn}\, u\,\mathrm{cn}\, u}{k'^2\,\mathrm{dn}\, u} - \frac{1}{k^2}\left[u - \frac{1}{k'^2}E(u)\right]\\
&\qquad\qquad \sim \frac{-\tau\sqrt{\xi^2 - \tau^2}}{k'^2\sigma\xi} - \frac{1}{k^2}\left[u_0 - \frac{1}{k'^2}E(u_0)\right] \quad \text{as } \lambda \to 0;\\
&\int_0^u \frac{\mathrm{sn}^2 u}{\mathrm{cn}^2 u}\, du = \frac{1}{k'^2}\left[\frac{\mathrm{sn}\, u\,\mathrm{dn}\, u}{\mathrm{cn}\, u} - E(u)\right] \sim \frac{1}{k'^2}\left[\frac{\sigma\sqrt{\xi^2 - \tau^2}}{\tau\xi} - E(u_0)\right] \quad \text{as } \lambda \to 0.
\end{aligned} \tag{59}$$

Here, $k'^2 = 1 - k^2$ is the complementary modulus. The first of equations 59 is obtained by using equations A2 and A5; the last two by using the periodic properties of the elliptic functions.

Numerical values for the elliptic integrals are calculated using the procedures given in the appendix: k and k' are known; equations A11 through A13 give the theta function parameters q and q' (these parameters have nothing to do with the angular velocity defined

in previous sections); equations A14 and A15 give the complete elliptic integrals; u and $E(u)$ are then obtained using one of the following sets of equations, depending on the value of q.

If $q \leq 0.09$,

$$\varsigma = \frac{1}{2q}\,\frac{\mathrm{dn}\,u - \sqrt{k'}}{\mathrm{dn}\,u + \sqrt{k'}} \tag{60}$$

and u is obtained from equations A8 and A19; equations A24 and A25 give:

$$E(u) = u\frac{E}{K} + \frac{k^2\,\mathrm{sn}\,u\,\mathrm{cn}\,u}{\mathrm{dn}\,u + \sqrt{k'}} - 8\frac{\pi}{2K}\,\frac{q^4 \sin\frac{\pi}{2K}4u}{1 + 2q^4\cos\frac{\pi}{2K}4u} + O\left(1000q^{16}\right). \tag{61}$$

If $q > 0.09$,

$$\varsigma' = \frac{1}{2q'}\,\frac{\mathrm{dn}\,u - \sqrt{k}\,\mathrm{cn}\,u}{\mathrm{dn}\,u + \sqrt{k}\,\mathrm{cn}\,u} \tag{62}$$

and u is obtained from equation A23; equation A28 gives:

$$E(u) = u\left(1 - \frac{E'}{K'}\right) + \frac{\mathrm{sn}\,u(k^2\,\mathrm{cn}\,u + \sqrt{k}\,\mathrm{dn}\,u)}{\mathrm{dn}\,u + \sqrt{k}\,\mathrm{cn}\,u} + 8\frac{\pi}{2K'}\,\frac{q'^4 \sinh\frac{\pi}{2K'}4u}{1 + 2q'^4\cosh\frac{\pi}{2K'}4u} + O\left(1000\varsigma'^8 q'^{16}\right). \tag{63}$$

Equations A19 and 61 are good as $k \to 0$ since $q \to 0$ at the same time. When $k \to 1$, $q \to 1$, which gives rise to the requirement for the q' series of equations A23 and 63. The cross-over point occurs when the maximum error in these last two equations equals that in the previous two. In equations A23 and 63, the maximum error occurs as $\varsigma' \to 1/2q'$. As can be seen by replacing q with 0.09 (and, therefore, q' with 0.016) in the error terms of the above equations, the maximum error for this worst case situation will only be $O\left(10^{-14}\right)$. Although this kind of accuracy is obviously not required in the final estimates of this report, it is useful for the calculation of equations 43 and 59 very close to the previously mentioned special case extremes, where the equations become indeterminate.

An elliptic disk: $\tau = 0$, $\xi > \sigma$

Only $\lambda = 0$ will be considered here since, realistically, only control surfaces (ie, secondary components) will ever need to be assigned zero thickness, and the flow field around secondary components need not be evaluated.

For the elliptic disk, some of the inertia coefficients of equations 43 become singular. As one might expect, they are $O(1/\tau)$, so that T (eq. 42) is finite when the singular t_{ii} are multiplied by the volume, V. The indeterminancy in the expressions for Vt_{ii} can be removed by expanding them in powers of τ. For this, the small τ expansions of the I's, eqs. 57 and 59 with $\lambda = 0$, must also be found. As $\tau \to 0$, one gets:

$$C \sim \frac{2\sigma\tau}{\xi^2} + O(\tau^3), \quad k^{-2} \sim \frac{\xi^2}{\xi^2 - \sigma^2} + O(\tau^2), \quad k'^{-2} \sim \frac{\xi^2}{\sigma^2} + O(\tau^2). \tag{64}$$

Then, making use of the fact that $u \to K$ and $E(u) \to E$ when $\lambda, \tau \to 0$:

$$\begin{aligned} I_1 &\sim \frac{2\sigma\tau}{\xi^2 - \sigma^2}(K - E) \\ I_2 &\sim \frac{2\sigma\tau}{\xi^2 - \sigma^2}\left(\frac{\xi^2}{\sigma^2}E - K\right) \\ I_3 &\sim 2 - \frac{2\tau}{\sigma}E. \end{aligned} \tag{65}$$

Thus, with reference to equations 43, if:

$$t'_{11} \equiv \frac{I_1}{2 - I_1}, \quad t'_{22} \equiv \frac{I_2}{2 - I_2}, \quad \ldots, \quad t'_{44} \equiv \frac{1}{5} \frac{(\sigma^2 - \tau^2)^2 (I_3 - I_2)}{2(\sigma^2 - \tau^2) + (\sigma^2 + \tau^2)(I_2 - I_3)}, \quad \ldots \tag{66}$$

then, as $\tau \to 0$, the Vt'_{ii} reduce to:

$$\begin{gathered} Vt'_{11} = 0, \quad Vt'_{22} = 0, \quad Vt'_{33} = \frac{4\pi\xi\sigma^2}{3E}, \\ Vt'_{44} = \frac{4\pi\xi\sigma^4(\xi^2 - \sigma^2)}{15\left[(2\xi^2 - \sigma^2)E - \sigma^2 K\right]}, \quad Vt'_{55} = \frac{4\pi\xi^3\sigma^2(\xi^2 - \sigma^2)}{15\left[(\xi^2 - 2\sigma^2)E + \sigma^2 K\right]}, \quad Vt'_{66} = 0. \end{gathered} \tag{67}$$

When $\xi \to \sigma$, the last of these expressions become indeterminate since then $k \to 0$ and $K \to E$. This case must be considered separately.

A circular disk: $\tau = 0$, $\xi = \sigma$

Again, $\lambda = 0$ only. Here it is simplest to go back to the case of the oblate spheroid (eqs. 53 and 54 with $\lambda = 0$) and let $\tau \to 0$, whence:

$$\begin{aligned} I_3 &\sim \left[2 + O(\tau^2)\right]\left[1 - \left(\frac{\tau}{\xi} + O(\tau^3)\right)\left(\frac{\pi}{2} + O(\tau)\right)\right] \sim 2 - \frac{\pi\tau}{\xi} + O(\tau^2) \\ I_1 &= I_2 \sim \frac{\pi\tau}{2\xi} + O(\tau^2). \end{aligned} \tag{68}$$

Thus:

$$Vt'_{11} = Vt'_{22} = 0, \quad Vt'_{33} = \tfrac{8}{3}\xi^3, \quad Vt'_{44} = Vt'_{55} = \tfrac{16}{45}\xi^5, \quad Vt'_{66} = 0. \tag{69}$$

Equations 69 are also derived by Lamb, but using a different method.

7 Analytical Expressions for the Added Masses of a Long Slender Ellipsoid

A submarine's hull length tends to be large relative to its transverse dimensions. This allows the expressions for the inertia coefficients of the previous section to be expanded in inverse powers of the largest principal axis length. One begins by expanding equation 56:

$$k^2 = 1 - \frac{\sigma^2 - \tau^2}{\xi^2} - \frac{\tau^2(\sigma^2 - \tau^2)}{\xi^4} + \cdots . \tag{70}$$

Since $k \to 1$ as $\xi \to \infty$, q' will be close to zero and the general case procedures for $q > 0.09$ should be followed (see equations 62 and 63). The next step is to obtain the expansion for $\sqrt{k}$ from equation 70, followed by that for $2\epsilon_0'$, q', etc. (eqs. A11 and A12). Eventually, one can show that, if $\Lambda \equiv \ln\big(4a/(c+b)\big)$, then:

$$\begin{aligned}
t_{11} &\sim \frac{bc}{a^2}(\Lambda - 1) + \frac{bc}{4a^4}\Big[\Lambda\big(4bc\Lambda + 3c^2 - 8cb + 3b^2\big) - 4c^2 + 7cb - 4b^2\Big] + \cdots \\
t_{22} &\sim \frac{c}{b} - \frac{c(c+b)}{4a^2 b}\big[2(c+b)\Lambda - c - 3b\big] \\
&\quad + \frac{c(c+b)}{64a^4 b}\Big\{4(c+b)\Lambda\big[4c(c+b)\Lambda - 7c^2 - 12cb - 9b^2\big] \\
&\qquad + 17c^3 + 25c^2 b + 51cb^2 + 51b^3\Big\} + \cdots \\
t_{33} &= t_{22}(a,c,b), \text{ where } t_{22} \equiv t_{22}(a,b,c). \\
t_{44} &\sim \frac{(c^2 - b^2)^2}{10bc}\left\{1 - \frac{(c+b)^2}{4a^2} + \frac{(c+b)^2}{64a^4}\big[12(c+b)^2\Lambda - 15c^2 - 26cb - 15b^2\big] + \cdots\right\} \\
t_{55} &\sim \frac{ba^2}{5c} - \frac{b}{20c}\big[6(c+b)^2\Lambda - 3c^2 - 20cb - 5b^2\big] \\
&\quad + \frac{b}{320a^2 c}\Big\{12(c+b)^2\Lambda\big[12b(c+b)\Lambda + c^2 - 60cb - 25b^2\big] \\
&\qquad + 3c^4 + 598c^3 b + 1468c^2 b^2 + 794cb^3 + 177b^4\Big\} + \cdots \\
t_{66} &= t_{55}(a,c,b), \text{ where } t_{55} \equiv t_{55}(a,b,c)
\end{aligned} \tag{71}$$

Equations 71 are particularly useful in showing how hull added masses are analytically related to hull geometry. For numerical calculations, one can expect the error in the expansions to be of the order of the first neglected term. Although extensive calculations have not been performed, the equations appear to give satisfactory engineering accuracy for $\ell/d > 6$; good accuracy is obtained for $\ell/d > 8$.

Since the present theory evaluates the t_{ii} exactly, it does not make direct use of equations 71.

8 Replacing a Component with its Best Fit Ellipsoid

This step is as important as any so far. Benefits from the analysis of the previous sections will be maximized if a submarine component is replaced by an ellipsoid whose geometry and position are optimally chosen (due consideration being given to the approximate nature of these estimations). The following analyses show the important characteristics this replacement should model.

A hull component

A hull component replacement ellipsoid will have its largest principal axis (length $2a$) parallel to the x axis of the conventional submarine body fixed axes. Its width and height are determined by the lengths of its other two principal axes, $2b$ and $2c$, which are parallel to the body y and z axes, respectively. All hull components are assumed to be symmetric about a vertical plane through their centerlines. This plane will be parallel to the x–z plane formed by the submarine body axes, but may be displaced from it by an amount $\bar{y}$. Although $\bar{y}$ will usually be zero for the main hull component, in general it will not be for, say, an outboard pod for which the 'hull component' representation is appropriate.

With $\Omega = \Phi = 0$, equations 23 simplify to:

$$
\begin{aligned}
X_{\dot{u}} &= -\rho V t_{11} \\
X_{\dot{q}} &= \bar{z} X_{\dot{u}} \\
X_{\dot{r}} &= -\bar{y} X_{\dot{u}} \\
Y_{\dot{v}} &= -\rho V t_{22} \\
Y_{\dot{p}} &= -\bar{z} Y_{\dot{v}} \\
Y_{\dot{r}} &= \bar{x} Y_{\dot{v}} \\
Z_{\dot{w}} &= -\rho V t_{33} \\
Z_{\dot{p}} &= \bar{y} Z_{\dot{w}} \\
Z_{\dot{q}} &= -\bar{x} Z_{\dot{w}}
\end{aligned}
\qquad
\begin{aligned}
K_{\dot{p}} &= -\rho V t_{44} + \bar{y}^2 Z_{\dot{w}} + \bar{z}^2 Y_{\dot{v}} \\
K_{\dot{q}} &= -\bar{x}\bar{y} Z_{\dot{w}} \\
K_{\dot{r}} &= -\bar{x}\bar{z} Y_{\dot{v}} \\
M_{\dot{q}} &= -\rho V t_{55} + \bar{z}^2 X_{\dot{u}} + \bar{x}^2 Z_{\dot{w}} \\
M_{\dot{r}} &= -\bar{y}\bar{z} X_{\dot{u}} \\
N_{\dot{r}} &= -\rho V t_{66} + \bar{x}^2 Y_{\dot{v}} + \bar{y}^2 X_{\dot{u}}
\end{aligned}
\qquad (72)
$$

Equations 71 show how sensitive these added mass terms are to variations in a, b, and c. When multiplied by $V = \frac{4}{3}\pi abc$, the lowest order terms in the expressions for t_{22}, t_{33}, t_{55}, and t_{66} are independent of the *dimension in the direction of motion* associated with the coefficients $Y_{\dot{v}}$, $Z_{\dot{w}}$, $M_{\dot{q}}$, and $N_{\dot{r}}$ respectively; this dimension has only a small affect on these added mass coefficients. In other words, modelling the characteristics of the maximum cross-sectional area perpendicular to the direction of motion is of primary importance to these four terms; modelling the volume is not important.

This is consistent with the expression for the added mass per unit length of an elliptic cylinder moving in a direction perpendicular to its longitudinal axis[2]:

$$\pi \rho b^2, \qquad (73)$$

where $2b$ is the length of the principal axis (of the cross-sectional ellipse) oriented perpendicular to the motion. The dimension parallel to the motion has absolutely no effect on this result.

One can use this 2-D result in a strip theory formulation of the added masses. If $B(x)$ is the local breadth of the hull component, $H(x)$ the local height as seen in a sheer profile, $\overline{H}(x)$ the z coordinate (in conventional body fixed axes) giving the midpoint of the local height line, and ℓ the length of the component, then strip theory formulations of the following added mass terms make use of the indicated integrals:

$$
\begin{aligned}
Y_{\dot{v}}: \quad & I_2 \equiv \int_\ell H^2(x)\,dx \doteq \frac{16}{3}ac^2 \\
Z_{\dot{w}}: \quad & I_3 \equiv \int_\ell B^2(x)\,dx \doteq \frac{16}{3}ab^2 \\
Y_{\dot{r}}, N_{\dot{v}}: \quad & I_{x2} \equiv \int_\ell xH^2(x)\,dx \doteq \bar{x}\frac{16}{3}ac^2 \\
Z_{\dot{q}}, M_{\dot{w}}: \quad & I_{x3} \equiv \int_\ell xB^2(x)\,dx \doteq \bar{x}\frac{16}{3}ab^2 \\
Y_{\dot{p}}, K_{\dot{v}}: \quad & I_x \equiv \int_\ell \overline{H}(x)H^2(x)\,dx \doteq \bar{z}\frac{16}{3}ac^2 \\
Vt_{55}: \quad & I_5 \equiv \int_\ell (x-\bar{x})^2B^2(x)\,dx \doteq \frac{16}{15}a^3b^2 \\
Vt_{66}: \quad & I_6 \equiv \int_\ell (x-\bar{x})^2H^2(x)\,dx \doteq \frac{16}{15}a^3c^2.
\end{aligned}
\tag{74}
$$

These I integrals are easily calculated from hull coordinates. The RHS's of the equations give the values of the integrals for an ellipsoid with its centroid located at $(\bar{x}, \bar{y}, \bar{z})$. Thus, the best fit hull replacement ellipsoid will be one that best satisfies equations 74. Note that X and K derivative characteristics do not contribute to this decision making process. This is because X derivatives are less important to submarine maneuvering characteristics than the cross-flow terms, and because Vt_{44} for the hull component is invariably dominated by the other terms and/or the sail's contribution to $K_{\dot{p}}$.

In the calculations that follow, $\bar{y}$ is assumed to be a known constant, determined by the location of the hull component. a, b, c, $\bar{x}$ and $\bar{z}$ are all unknown and are calculated from the information provided about the hull component, as summarized in the I integrals. The problem, of course, is that there are seven equations in five unknowns. This is resolved as follows.

$\bar{z}$ can be calculated directly:

$$\bar{z} = I_x/I_2\,. \tag{75}$$

$\bar{x}$ is taken to be the average of its horizontal and vertical plane predictions:

$$\bar{x} = (I_{x3}/I_3 + I_{x2}/I_2)/2 \tag{76}$$

and the errors associated with this approximation are monitored with:

$$\epsilon_x \equiv (\bar{x} - I_{x2}/I_2)/\ell = -(\bar{x} - I_{x3}/I_3)/\ell\,. \tag{77}$$

Ellipsoid semi-axis lengths a, b, and c are determined by the remaining four of equations 74, by minimizing the sum of the squares of the errors with which the equations are satisfied. Let:

$$\epsilon_2 \equiv \frac{16}{3I_2}ac^2 - 1\,, \quad \epsilon_3 \equiv \frac{16}{3I_3}ab^2 - 1\,, \quad \epsilon_5 \equiv \frac{16}{15I_5}a^3b^2 - 1\,, \quad \epsilon_6 \equiv \frac{16}{15I_6}a^3c^2 - 1\,. \tag{78}$$

Then, if $\Sigma \equiv \epsilon_2^2 + \epsilon_3^2 + \epsilon_5^2 + \epsilon_6^2$, the three equations determining a, b, and c are:

$$\frac{\partial \Sigma}{\partial a} = 0\,, \quad \frac{\partial \Sigma}{\partial b} = 0\,, \quad \frac{\partial \Sigma}{\partial c} = 0\,. \tag{79}$$

There results:

$$\epsilon_2 = \epsilon_5\,, \quad \epsilon_3 = \epsilon_6\,, \quad \epsilon_3(1+\epsilon_3) = -\epsilon_5(1+\epsilon_5) \tag{80}$$

so that:

$$a = \left(\frac{25I_5I_6}{I_2I_3}\right)^{1/4}, \quad c = b\left(\frac{I_2I_6}{I_3I_5}\right)^{1/4}, \quad b^2 = \frac{3I_3}{16a}\,\frac{1+\sqrt{I_3I_6/(I_2I_5)}}{1+I_3I_6/(I_2I_5)}\,. \tag{81}$$

Equations 75, 76, and 81 define the best fit hull replacement ellipsoid.

Now, consider the added moment of inertia per unit length for a rolling elliptic cylinder, which is[2]:

$$\pi\rho\left(c^2 - b^2\right)^2/8\,. \tag{82}$$

Strip theory makes use of this equation in formulating the following integral, which is used for calculating $K_{\dot{p}}$:

$$Vt_{44}\colon \quad I_4 \equiv \int_\ell \left[H^2(x) - B^2(x)\right]^2 dx \doteq \frac{256}{15}a(c^2-b^2)^2\,. \tag{83}$$

Here, again, the RHS of this equation is the value of the integral for the hull replacement ellipsoid. The degree to which equation 83 is satisfied is monitored by:

$$\epsilon_4 \equiv \frac{256}{15I_4}a(c^2-b^2)^2 - 1\,. \tag{84}$$

What one really wants to do is monitor the errors in equations 72 compared to the *total* added masses (written as $(\ )_T$) for the complete vehicle configuration. This can be done by monitoring the following relative errors:

$$\begin{aligned}
\epsilon_Y &\equiv \epsilon_2 Y_{\dot{v}}/(Y_{\dot{v}})_T \\
\epsilon_Z &\equiv \epsilon_3 Z_{\dot{w}}/(Z_{\dot{w}})_T \\
\epsilon_K &\equiv \left(\frac{-\epsilon_4}{1+\epsilon_4}Vt_{44} + \bar{y}^2\epsilon_3 Z_{\dot{w}} + \bar{z}^2\epsilon_2 Y_{\dot{v}}\right)\Big/(K_{\dot{p}})_T \\
\epsilon_M &\equiv (-\epsilon_5 Vt_{55} + \bar{x}^2\epsilon_3 Z_{\dot{w}} - 2\bar{x}\epsilon_x \ell Z_{\dot{w}})/(M_{\dot{q}})_T \\
\epsilon_N &\equiv (-\epsilon_6 Vt_{66} + \bar{x}^2\epsilon_2 Y_{\dot{v}} + 2\bar{x}\epsilon_x \ell Y_{\dot{v}})/(N_{\dot{r}})_T\,.
\end{aligned} \tag{85}$$

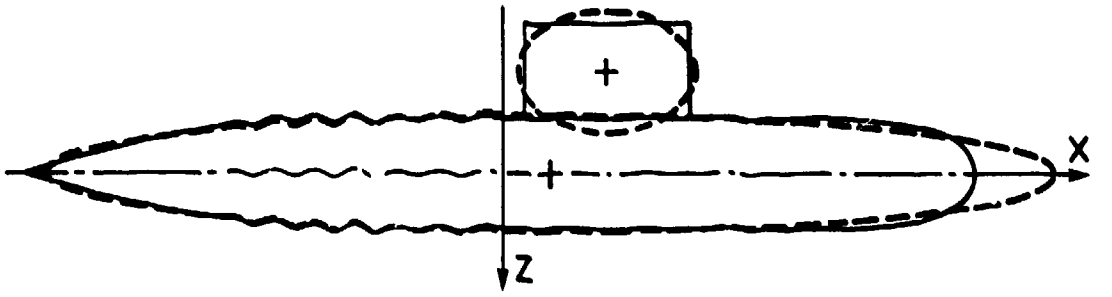

a) *Axisymmetric hull.*

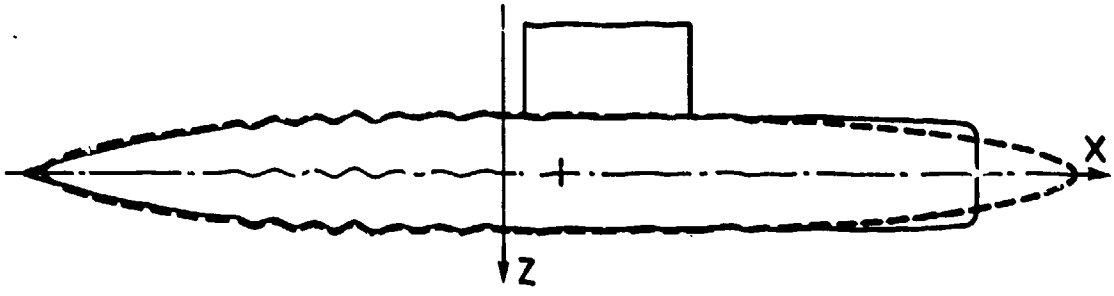

b) *Asymmetric hull with straight vertical stem.*

Figure 1 *Sheer plans for two standard hulls and sail with their replacement ellipsoids. The hulls have identical breadth plans.*

Here, it is understood that the added masses in the numerators of these expressions are those for the hull component; also, except for ϵ_4, the ϵ_i are assumed to be small. These expressions estimate the relative errors in the overall added masses resulting from fitting an asymmetric hull component with a single ellipsoid. For axisymmetric hull components, the ϵ_i are all zero since then equations 74 reduce to four equations in four unknowns, and these can be satisfied exactly.

Figure 1 shows the sheer plans of two different submarine hulls, along with their best fit ellipsoids. The asymmetry in the hull of Figure 1b is confined to the nose section, the front 20 percent of the hull length.

For the asymmetric hull, ϵ values are:

$$\epsilon_2 = 0.019, \quad \epsilon_3 = -0.020, \quad \epsilon_4 = -0.67, \quad \epsilon_x = -0.009$$

and for the hull and sail combination shown:

$$\epsilon_Y = 0.016, \quad \epsilon_Z = -0.020,$$
$$\epsilon_K = -0.003, \quad \epsilon_M = 0.019, \quad \epsilon_N = -0.019.$$

Note the extremely small effect the very large ϵ_4 value has on ϵ_K; this is because of the large contribution to $K_{\dot{p}}$ from the sail. This asymmetric hull gave the largest $\epsilon_2, \epsilon_3, \epsilon_4$ values of any hull tested. This is most likely due to the hull's asymmetry being all at one end, while the ellipsoid modelling it is evenly asymmetric over its entire length.

Equations 81 are responsible for these low ϵ values. An initial attempt at reducing equations 74 to five equations in five unknowns was made by assuming $B(x)/H(x) = b/c$ for all x,

and using I_4 to determine the difference between b and c; however, this resulted in ϵ values as large as 0.05, even though ϵ_4 was very small.

Section 10 gives an example of another hullform.

An appendage

Three types of appendages will be considered, as shown in Figure 2. Most appendages, and certainly the sail, will need to be represented by a type I or II appendage. The type III appendage could be useful for modelling sailplanes or, perhaps, endplates. It should not be used to model a pair of appendages separated by the hull if interference effects are also being modelled, since the centroid of the replacement ellipsoid would then lie within the hull and the interference velocity at this centroid would have no meaning.

The specifications required to completely determine the geometry and location of each type of control surface are:

$$\text{Types I \& II: } (x_1, y_1, z_1),\ \Phi,\ (\hat{x}_2, \hat{y}_2),\ (\hat{x}_3, \hat{y}_3),\ (\hat{x}_4, \hat{y}_4),\ t$$
$$\text{Type III: } (x_1, y_1, z_1),\ \Phi,\ c_1,\ (\hat{x}_4, \hat{y}_4),\ c_4,\ (\hat{x}_5, \hat{y}_5),\ c_5,\ t.$$

For each type, (x_1, y_1, z_1) are the body axis coordinates of the trailing edge at the root of the appendage. This point is also the origin of the local $\hat{x}, \hat{y}, \hat{z}$ axes. The $\hat{x}$ axis is always aligned with, though usually displaced from, the body x axis. Φ is the angle the $\hat{y}$ axis must roll away from the body fixed y axis to bring itself into the plane of the appendage. $(\hat{x}_i, \hat{y}_i, 0)$, $i = 2,3,4,5$, are the corner coordinates of the appendages in the local $\hat{x}, \hat{y}, \hat{z}$ coordinate system; they determine Ω. (For the type III appendage, root and tip cord lengths are specified instead of leading edge coordinates.) Together, Φ and Ω give the orientation of the μ, ν axes, and of the x', y', z' axes. As discussed in Section 2, Φ and Ω are zero when the y' and x' axes are aligned with the body fixed y and x axes, respectively; positive rotations are determined by the Right Hand Rule, with a rotation in Φ being applied before that in Ω. The thickness to chord ratio of the appendage is designated by t.

The centroids of the ellipsoids replacing these configurations are located at $(\bar{\mu}, \bar{\nu})$, as discussed below. These points locate the origins of the x', y' axes, which are aligned with, though displaced from, the μ, ν axes.

Note that the μ, ν axes defined in this section have nothing to do with the confocal ellipsoidal coordinates presented in Section 4.

For type I, Ω is determined by taking the ν axis to be parallel to the bisector of the angle formed by the leading and trailing edges of the appendage. The y' axis, also parallel to this bisector, is allowed to be displaced from it to partially account for asymmetric end geometries. This type I representation can also be used for triangular fins in which the points $(\hat{x}_3, \hat{y}_3)$ and $(\hat{x}_4, \hat{y}_4)$ are coincident.

For type II, the μ axis is simply taken to be the line joining the leading and trailing edge root coordinates; that is, $\Omega = \tan^{-1}(\hat{y}_2/\hat{x}_2)$. Everything else is the same as type I. Since this type II representation does not require leading and trailing edges in order to calculate Ω, it can accomodate all kinds of triangular fins, including those in which the points $(\hat{x}_2, \hat{y}_2)$ and $(\hat{x}_3, \hat{y}_3)$ or $(\hat{x}_4, \hat{y}_4)$ and $(0,0)$ are coincident.

For type III, the simplification of setting $\Omega = 0$ is made. This type partially accounts for asymmetries in the appendages about the μ axis and the line $\mu = c_1/2$ by strategically locating the ellipsoid's centroid.

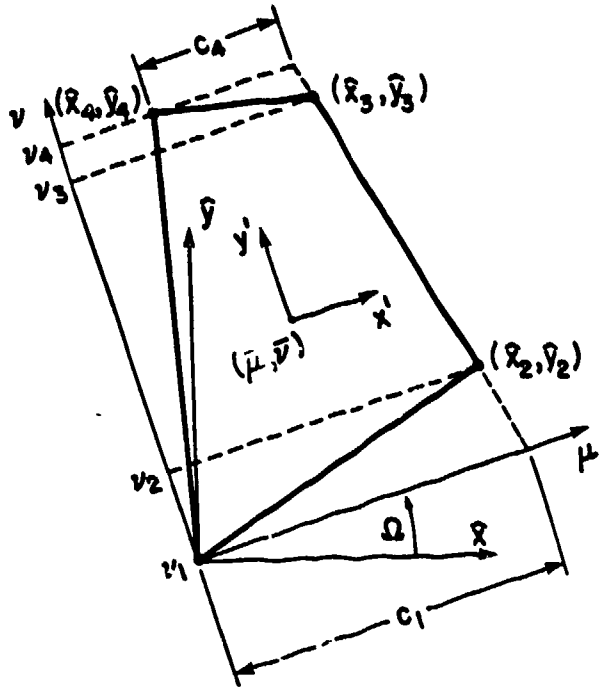

Type I: Ω *determined by bisector.*

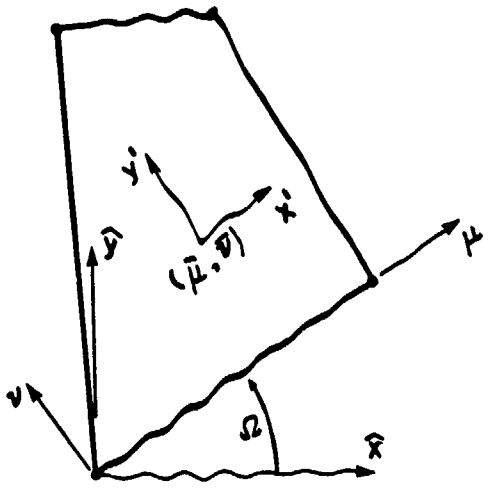

Type II: $\Omega = \tan^{-1}(\hat{y}_2/\hat{x}_2)$.

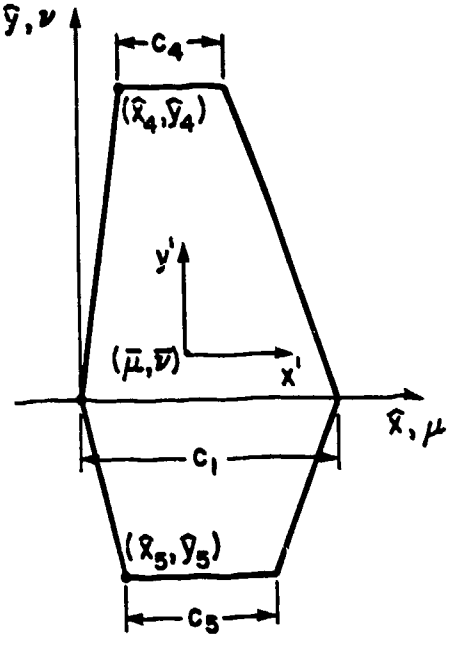

Type III: $\Omega = 0$.

Figure 2 *Appendage profiles in the plane* $x', z \approx 0$.

To choose the optimum dimensions and position of a replacement ellipsoid, one identifies those characteristics which are most desirable to model. Unlike the hull, where simultaneously monitoring motions in four or all of the degrees of freedom is appropriate, an appendage primarily affects forces perpendicular to its planform area. This suggests three degrees of freedom are important: translation along the x' axis and rotations about the x' and y' axes. However, only the first two of these are of *primary importance* because of the very important role appendages play in vehicle rolling motions (this assumes Ω is not large). Properly modelling the thickness of the appendage is not important when modelling these motions. Of course, having determined ellipsoid geometry, the added masses for all degrees of freedom will be calculated.

If $c(\nu)$ is the local chord length (perpendicular to the ν axis) of a type I, II, or III appendage and $\bar{c}(\nu)$ is the μ coordinate of the midpoint of the local chord length, then the force and moment characteristics that a replacement ellipsoid should model are:

$$\begin{aligned} J_0 &\equiv \int_S c^2(\nu)\,d\nu = \tfrac{16}{3}a^2b\,, & J_{\nu 1} &\equiv \int_S \nu c^2(\nu)\,d\nu = \bar{\nu}\tfrac{16}{3}a^2b\,, \\ J_{\mu 1} &\equiv \int_S \bar{c}(\nu)c^2(\nu)\,d\nu = \bar{\mu}\tfrac{16}{3}a^2b\,, & J_{\nu 2} &\equiv \int_S \nu^2 c^2(\nu)\,d\nu = \tfrac{16}{15}a^2b^3 + \bar{\nu}^2\tfrac{16}{3}a^2b\,. \end{aligned} \tag{86}$$

These integrals model the distribution of the square of the chord length along the span (S) of the appendage, which equation 73 indicates to be an important two-dimensional added mass characteristic of the cross-flows resulting from the translation and rotation of *primary importance*. The righthand sides of the equations give the results of the integrals for an ellipsoid with its principal axes aligned with the x', y', z' axes and its centroid at $(\bar{\mu}, \bar{\nu})$.

The following equations give the expressions that are used for $c(\nu)$ and $\bar{c}(\nu)$ in the above integrals:

$$\text{Types I \& II} \begin{cases} c(\nu) = \dfrac{\nu-\nu_a}{\nu_b-\nu_a}c_b\,, & \bar{c}(\nu) = \dfrac{c_1}{2} + \dfrac{\nu-\nu_b}{\nu_2}\dfrac{c_a}{2}\,, & \nu_a \le \nu \le \nu_b \\ c(\nu) = c_b - \dfrac{\nu-\nu_b}{\nu_c-\nu_b}(c_b-c_c)\,, & \bar{c}(\nu) = \dfrac{c_1}{2}\,, & \nu_b \le \nu \le \nu_c \\ c(\nu) = \dfrac{\nu_d-\nu}{\nu_d-\nu_c}c_c & \bar{c}(\nu) = \dfrac{c_1}{2} + \dfrac{\nu_c-\nu}{\nu_4-\nu_3}\dfrac{c_d}{2}\,, & \nu_c \le \nu \le \nu_d \end{cases} \tag{87}$$

$$\text{Type III} \begin{cases} c(\nu) = c_1 - \dfrac{c_1-c_5}{\hat{y}_5}\nu\,, & \bar{c}(\nu) = \dfrac{c_1}{2} + \dfrac{2\hat{x}_5+c_5-c_1}{2\hat{y}_5}\nu\,, & \hat{y}_5 \le \nu \le 0 \\ c(\nu) = c_1 - \dfrac{c_1-c_4}{\hat{y}_4}\nu\,, & \bar{c}(\nu) = \dfrac{c_1}{2} + \dfrac{2\hat{x}_4+c_4-c_1}{2\hat{y}_4}\nu\,, & 0 \le \nu \le \hat{y}_4 \end{cases}$$

where, for types I and II: ν_a and ν_b are the minimum and maximum of ν_1 and ν_2, respectively, ν_c and ν_d are the minimum and maximum of ν_3 and ν_4, respectively, and c_i is the chord length perpendicular to the ν axis at $\nu = \nu_i$. Thus, the type I and II representation allows ν_2 to be greater than or less than zero, and ν_4 to be greater than or less than ν_3. The type I representation cannot be used if it results in ν_c being less than ν_b; type II must be used instead.

For a type I or II appendage, the limits of integration in equations 86 are from ν_a to ν_d. One gets:

$$
\begin{aligned}
J_0 &= [c_c^2(\nu_d-\nu_b) + c_c c_b(\nu_c-\nu_b) + c_b^2(\nu_c-\nu_a)]/3 \\
J_{\mu 1} &= \frac{c_1}{2}J_0 - [c_d c_c^2(\nu_4-\nu_3) + c_b^2 c_a \nu_2]/2 \\
J_{\nu 1} &= [c_c^2(\nu_d-\nu_b)(\nu_d+2\nu_c+\nu_b) + 2c_c c_b(\nu_c^2-\nu_b^2) + c_b^2(\nu_c-\nu_a)(\nu_c+2\nu_b+\nu_a)]/12 \\
J_{\nu 2} &= [c_c^2(\nu_d-\nu_b)(\nu_d^2+2\nu_d\nu_c+\nu_d\nu_b+3\nu_c^2+2\nu_c\nu_b+\nu_b^2) + c_c c_b(\nu_c-\nu_b)(3\nu_c^2+4\nu_c\nu_b+3\nu_b^2) \\
&\quad + c_b^2(\nu_c-\nu_a)(\nu_c^2+2\nu_c\nu_b+\nu_c\nu_a+3\nu_b^2+2\nu_b\nu_a+\nu_a^2)]/30 .
\end{aligned}
\tag{88}
$$

For a type III appendage, the limits of integration are from $\hat{y}_5$ to $\hat{y}_4$:

$$
\begin{aligned}
J_0 &= [(c_1^2+c_1c_4+c_4^2)\hat{y}_4 - (c_1^2+c_1c_5+c_5^2)\hat{y}_5]/3 \\
J_{\mu 1} &= \frac{c_1}{2}J_0 + [(c_1^2+2c_1c_4+3c_4^2)(2\hat{x}_4+c_4-c_1)\hat{y}_4 - (c_1^2+2c_1c_5+3c_5^2)(2\hat{x}_5+c_5-c_1)\hat{y}_5]/24 \\
J_{\nu 1} &= [(c_1^2+2c_1c_4+3c_4^2)\hat{y}_4^2 - (c_1^2+2c_1c_5+3c_5^2)\hat{y}_5^2]/12 \\
J_{\nu 2} &= [(c_1^2+3c_1c_4+6c_4^2)\hat{y}_4^3 - (c_1^2+3c_1c_5+6c_5^2)\hat{y}_5^3]/30 .
\end{aligned}
\tag{89}
$$

Finally, for each type of control surface:

$$
\bar{\mu} = \frac{J_{\mu 1}}{J_0}, \quad \bar{\nu} = \frac{J_{\nu 1}}{J_0}, \quad b^2 = 5\left(\frac{J_{\nu 2}}{J_0} - \bar{\nu}^2\right), \quad a^2 = \frac{3J_0}{16b} . \tag{90}
$$

The ellipsoid principal semi-axis length along the x' axis, c, can be chosen without compromising the above more important calculations. If t is the thickness to chord ratio of the control surface, then the following equation models the distribution of the square of the thickness perpendicular to the μ–ν plane.

$$
\int [tc(\nu)]^2 \, d\nu = \tfrac{16}{3} c^2 b .
$$

Here, again, the right hand side is the value of the integral for an ellipsoid. However, this integral is just equal to $t^2 J_0$. Thus, for types I, II, and III:

$$
c = ta . \tag{91}
$$

Figure 3 shows the replacement ellipsoids for two of the appendages shown in Figure 2. Figure 1 shows the replacement ellipsoid for a sail.

To locate the appendages (ie, obtain $\mathbf{r}$) one requires the inverse (which equals the transpose) of the B matrix, eq. 13:

$$
\mathbf{r} \equiv \begin{pmatrix} \bar{x} \\ \bar{y} \\ \bar{z} \end{pmatrix} = \begin{pmatrix} x_1 \\ y_1 \\ z_1 \end{pmatrix} + \mathbf{B}^T \begin{pmatrix} \bar{\mu} \\ \bar{\nu} \\ 0 \end{pmatrix} .
$$

Thus:

$$
\begin{aligned}
\bar{x} &= x_1 + \bar{\mu}\cos\Omega - \bar{\nu}\sin\Omega \\
\bar{y} &= y_1 + \bar{\mu}\sin\Omega\cos\Phi + \bar{\nu}\cos\Omega\cos\Phi \\
\bar{z} &= z_1 + \bar{\mu}\sin\Omega\sin\Phi + \bar{\nu}\cos\Omega\sin\Phi .
\end{aligned}
\tag{92}
$$

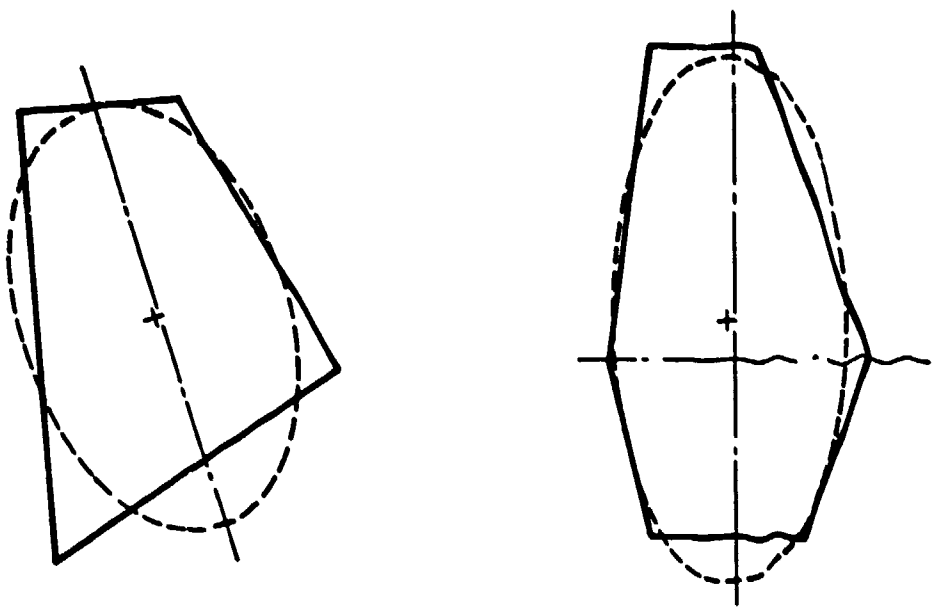

Type I *Type III*

Figure 3 *Replacement ellipsoids for two of the appendages of Figure 2.*

Unlike some methods[5], the present theory does not account for asymmetric end effects on an appendage. These effects are due to the flow around the tip being different from that around the root. The proper way of accounting for this is by analysing the flow around the appendage plus its image in the hull, and calculating the forces only on that portion of the 'extended' appendage which protrudes into the fluid. However, this would have required a major alteration to the present theory, which is as simple as it is only because the added mass coefficients can be related to the total energy in the flow. If it were necessary to calculate the force on only a portion of an ellipsoid, then the complexity of the appendage analysis would increase substantially.

This criticism is moderated by the present method's de-emphasis of end effects. The integrals of equations 86 are only concerned with 2-D aspects of the flow normal to the appendage. This results in a replacement ellipsoid with a larger geometric aspect ratio than the original appendage. For example, the replacement ellipsoid for an appendage with a square planform has $b/a = 1.2$.

9 Optimizing Hull Ellipsoid Geometry for Interference Velocity Calculations

The interference velocity at an appendage is determined by the geometry of the hull replacement ellipsoid. In the previous section, this geometry was chosen as the best fit to the *overall* hull geometry. However, the interference velocity is largely dependent on the *local* hull geometry opposite the appendage. This section describes the way in which the hull replacement ellipsoid geometry is modified to best represent the local geometry opposite the centroid of an appendage's replacement ellipsoid prior to calculating the interference velocity at that centroid.

A result of slender body theory is that axial disturbance velocities over a slender hull are of a smaller order of magnitude than transverse disturbance velocities. The transverse velocities are primarily determined by the local cross-sectional hull profile, while the axial velocities are related to the local slopes of the longitudinal profiles. Ideally, the optimized hull ellipsoid would model all of these local characteristics, but compromises must be made. Since axial interference velocities are small, no attempt is made to match the local longitudinal profile slopes; such matching also often results in a dramatic reduction in the length of the original hull replacement ellipsoid, so that end effects may then adversely affect the more important transverse velocity predictions. The usual compromise that the cross-sectional profile of the hull ellipsoid will be elliptical, regardless of the true hull profile, is also made.

The optimisation procedure proceeds as follows. To improve the prediction of local transverse velocities, the transverse dimensions of the original hull replacement ellipsoid are adjusted so that the local breadth and sheer profile coordinates of the hull (obtained by linear interpolation between the specified profile coordinates) are exactly matched. In general, this requires adjustments to the hull ellipsoid parameters b, c, and $\mathbf{z}$. For the longitudinal direction, a is only adjusted in those instances when the appendage is too close to the stern of the hull ellipsoid, as described below; $\mathbf{z}$ is never changed.

In some cases, the aft end of the original hull replacement ellipsoid may be too far forward to allow the local hull geometry opposite the tail appendages to be satisfactorily represented with the above modification. Where this occurs, a is usually increased in order to make the modified hull ellipsoid terminate aft of the appendage. Then the transverse dimensions of the ellipsoid are adjusted to match the hull profile coordinates opposite the appendage (see Figure 5 in the next section). This usually provides a good local fit at the tail but results in a somewhat narrower overall ellipsoid, which is not a problem since this modified hull ellipsoid is only used to calculate interference velocities at the tail.

If there are cases where an aft appendage is very close to or even aft of the end of the actual hull, a is only lengthened until the end of the hull ellipsoid is within a distance d of the actual hull end; a is left unchanged if it is already within this distance. Trial and error has shown that a good value for d is 2 percent of the hull length. The newly lengthened (or not) hull ellipsoid is then matched to the local hull profile coordinates at least a distance d ahead of its end, further forward if the appendage is forward of this location.

If the end of the original hull replacement ellipsoid is aft of the end of the actual hull (a very unusual situation), and if the appendage is very close to or aft of the end of the actual hull, no change is made to the original hull ellipsoid.

At the bow, the original hull replacement ellipsoid will usually extend out beyond the actual hull, as Figure 1 shows. As the presence of appendages very close to the bow is unusual, no attempt has been made to optimize the hull ellipsoid for such a case. If an appendage is

within a distance d of or off the forward end of either the actual hull or the original hull replacement ellipsoid, no modifications are made; otherwise, the transverse hull ellipsoid geometry is optimized as for any appendage well within the ends.

10 An Example

A computer program (called ESAM: Estimate Submarine Added Masses) has been developed which applies the calculations described in this report to submarine configurations. Appendix B describes its use and gives example input and output data files for the generic submarine configuration shown in Figure 4. Input data must contain the hull sheer and breadth plan coordinates, appendage geometry, and basic information about reference axes. The program automatically calculates replacement ellipsoid geometry and outputs this information together with a complete set of added mass predictions. For a complete submarine configuration, consisting of a hull and 7 appendages, the program takes about 2 seconds of CPU time on a VAX 11/750.

As well as sketching the submarine's longitudinal profiles, Figure 4 shows the size and location of the best fit hull replacement ellipsoid. Figure 5 shows how this ellipsoid is modified by ESAM for the purpose of calculating interference velocities at the rudder. These replacement ellipsoid geometries, along with those of all the other components, are listed in the output file of Appendix B.

The ϵ values for this hullform are:

$$\epsilon_2 = -0.013\,, \quad \epsilon_3 = 0.013\,, \quad \epsilon_4 = -0.35\,, \quad \epsilon_x = 0.005$$

and for the entire configuration:

$$\epsilon_Y = -0.012\,, \quad \epsilon_Z = 0.013\,,$$
$$\epsilon_K = -0.022\,, \quad \epsilon_M = -0.012\,, \quad \epsilon_N = 0.012\,.$$

Values of ϵ as large as 0.04 were obtained when the assumption $B(x)/H(x) = b/c$ was used instead of equations 81. The asymmetry in this hull is more evenly distributed over its length, and this results in generally lower ϵ values than for the previous hullform; however, the asymmetry is also quite large, so that ϵ_4 has a relatively large affect on ϵ_K.

Table 1 summarizes the added masses for the complete submarine. For comparison purposes, the table also shows the predictions when hull interference velocities are not considered and appendage thicknesses are set to zero. These conditions are all easily modelled by making simple parameter changes in the ESAM input file (interference effects are eliminated by assigning all appendages neutral *orders*). The prime over a coefficient indicates nondimensionalization.

The following discussion deals with the added mass terms on an individual basis. Note that alternating coefficients in Table 1 must be zero because of the submarine's symmetry about a longitudinal vertical plane, and since $\bar{y}_{\text{hull}} = 0$. ESAM does not assume such symmetry exists.

For this submarine, over 20 percent of the magnitude of $X_{\dot{u}}$ is due to appendage thickness. The sail is most responsible for this; although its section profile is rather thick (30 percent), its span is not large compared to some configurations.

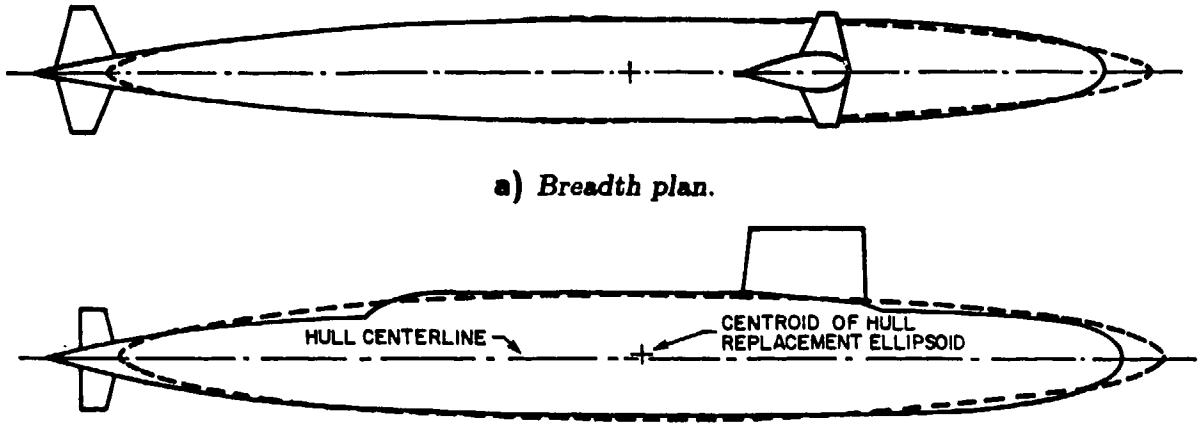

a) *Breadth plan.*

b) *Sheer plan.*

Figure 4 *Generic submarine and hull replacement ellipsoid.*

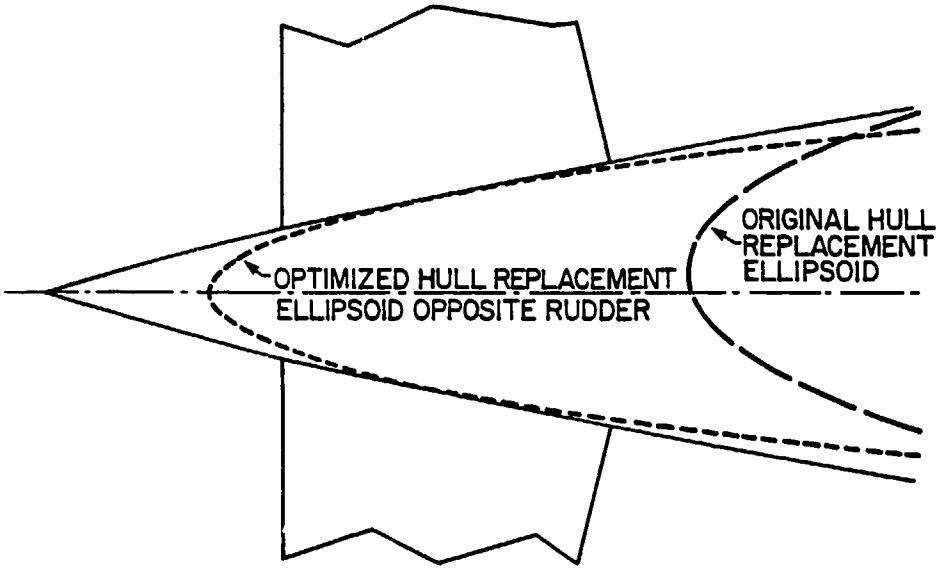

Figure 5 *Elevation view of original and optimized hull replacement ellipsoids opposite the rudder; the optimized ellipsoid is only used for calculating interference velocites at the centroids of the rudder replacement ellipsoids.*

Condition	1 Complete Theory	2 No Interference	3 No Appendage Thickness	4 Both (2) and (3)
$X'_{\dot{u}}$	−0.000305	−0.000303	−0.000236	−0.000236
$X'_{\dot{v}}, Y'_{\dot{u}}$	0.0	0.0	0.0	0.0
$X'_{\dot{w}}, Z'_{\dot{u}}$	−0.00000331	0.00000278	−0.00000138	0.0
$X'_{\dot{p}}, K'_{\dot{u}}$	0.0	0.0	0.0	0.0
$X'_{\dot{q}}, M'_{\dot{u}}$	0.00000504	0.00000539	0.00000087	0.00000062
$X'_{\dot{r}}, N'_{\dot{u}}$	0.0	0.0	0.0	0.0
$Y'_{\dot{v}}$	−0.0125	−0.0120	−0.0126	−0.0121
$Y'_{\dot{w}}, Z'_{\dot{v}}$	0.0	0.0	0.0	0.0
$Y'_{\dot{p}}, K'_{\dot{v}}$	−0.0000929	−0.0000753	−0.0000989	−0.0000796
$Y'_{\dot{q}}, M'_{\dot{v}}$	0.0	0.0	0.0	0.0
$Y'_{\dot{r}}, N'_{\dot{v}}$	−0.0000805	−0.0000314	−0.0000935	−0.0000395
$Z'_{\dot{w}}$	−0.00907	−0.00910	−0.00904	−0.00901
$Z'_{\dot{p}}, K'_{\dot{w}}$	0.0	0.0	0.0	0.0
$Z'_{\dot{q}}, M'_{\dot{w}}$	−0.0001021	−0.0000583	−0.0001130	−0.0000764
$Z'_{\dot{r}}, N'_{\dot{w}}$	0.0	0.0	0.0	0.0
$K'_{\dot{p}}$	−0.00000463	−0.00000451	−0.00000507	−0.00000493
$K'_{\dot{q}}, M'_{\dot{p}}$	0.0	0.0	0.0	0.0
$K'_{\dot{r}}, N'_{\dot{p}}$	−0.00000917	−0.00000680	−0.00001004	−0.00000744
$M'_{\dot{q}}$	−0.000434	−0.000423	−0.000435	−0.000422
$M'_{\dot{r}}, N'_{\dot{q}}$	0.0	0.0	0.0	0.0
$N'_{\dot{r}}$	−0.000541	−0.000525	−0.000543	−0.000526

Table 1 *Added mass predictions for the submarine of Figure 4. Column 1 presents the predictions of the complete theory (component contributions to these values are shown in the output file of Appendix B); column 2 neglects interference effects; column 3 sets all appendage thicknesses to zero; column 4 neglects both interference effects and appendage thicknesses. Coefficients are with respect to an origin located on the hull centerline opposite the centroid of the hull replacement ellipsoid.*

Table 1 shows how $X_{\dot{w}}$ is entirely dependent on the modelling of both interference effects and appendage thickness. The present theory models the hull with an ellipsoid, which has horizontal and vertical-transverse planes of symmetry not matched by the actual hull. It predicts that the hull makes no contribution to $X_{\dot{w}}$ when, in fact, one would expect a small contribution to be present. The size of such a contribution is unknown. However, the sensitivity of $X_{\dot{w}}$ to small asymmetries, such as the negative sweepback of the sail ($\Omega_{sail} = -3.3°$), can be determined: when Ω_{sail} is set to zero, the magnitude of $X_{\dot{w}}$ changes by 57 percent. For this submarine configuration, then, the current $X_{\dot{w}}$ prediction may only be an order of magnitude estimate. For configurations with hullforms more closely exhibiting the symmetries of an ellipsoid, the prediction of $X_{\dot{w}}$ might be better.

$X_{\dot{q}}$ is essentially determined by sail thickness, with interference effects being of secondary importance. The contribution to $X_{\dot{q}}$ from the hull (which is nonzero because the hull centroid is displaced upwards from the hull centerline) is an order of magnitude less than that from the sail.

Note that 4 percent of the value of $Y_{\dot{v}}$ is due to interference effects. These effects increase the sail's contribution to $Y_{\dot{v}}$ by 85 percent. Table 2 compares the present theory's predictions of the sail's contribution to $Y_{\dot{v}}$ to the theories mentioned in the Introduction (which account for neither hull interference velocities nor appendage thickness; Aucher models the sail's image in the hull while Humphreys and Watkinson do not).

Present Theory			Humphreys and Watkinson[4]	Aucher[5]
complete	without interference	neither thickness nor interference		
9.7	5.2	5.8	5.2	6.0

Table 2 *The contribution to* $10^4 Y'_{\dot{v}}$ *of the sail of Figure 4.*

$Y_{\dot{r}}, N_{\dot{v}}$ and $Z_{\dot{q}}, M_{\dot{w}}$ are difficult to predict accurately if they are referenced to a point close to the center of buoyancy (CB). This is because they are being estimated in the region of their zeros (which, incidently, are only approximately at the CB). Of more importance is the prediction of $Y_{\dot{r}}/Y_{\dot{v}}$, $N_{\dot{v}}/Y_{\dot{v}}$, $-Z_{\dot{q}}/Z_{\dot{w}}$, and $-M_{\dot{w}}/Z_{\dot{w}}$, the longitudinal locations of the zeros of the coefficients.

Although Table 1 shows very little change in $Z_{\dot{w}}$ for the various conditions, somewhat larger, partially compensating changes are occuring in the component contributions to it. For example, properly accounting for interference effects (ie, going from column 2 to column 1) roughly cuts in half the contributions from the sail (due to its thickness) and the sailplanes, while at the same time increasing by a third the contributions from the sternplanes. The effects of accounting for thickness and interference are more easily appreciated in the changes that result in $M_{\dot{w}}$, since $M_{\dot{w}}$ is sensitive to the longitudinal location at which these changes take place.

The K derivatives are dominated by the presence of the sail. Although the hull accounts for a third of the value of $K_{\dot{v}}$, it accounts for less than 10 percent of $K_{\dot{p}}$ and makes no contribution to $K_{\dot{r}}$. The cross-flow velocities associated with $\dot{v}$ and $\dot{r}$ result in large interference velocity effects in the sail's contribution to $K_{\dot{v}}$ and $K_{\dot{r}}$, but not as large as one might expect (cf, equations 29).

11 Conclusions

A theory for predicting all the added mass coefficients for a multi-component, deeply submerged vehicle has been presented. A program applying this theory to conventional submarine shapes gives very rapid numerical predictions of the coefficients. In keeping with the way most current experimental investigations of these characteristics are carried out, the theory ignores both the incidence of the vehicle to the oncoming flow and time in an unsteady flow.

Added masses are calculated by summing up the contributions from replacement ellipsoids optimally sized and positioned to best represent each body component. The hull replacement ellipsoid is given special attention; it is sized in such a way that errors associated with the replacement are minimized.

The theory accounts for both appendage thickness and hull interference velocities at appendages. Modelling these characteristics is shown to be necessary if reasonable predictions of the 'off-diagonal' added mass coefficients, responsible for at least some degree of coupling between motions in different degrees of freedom, are to be made. In addition, these characteristics are responsible for changes to five of the principal (ie, 'diagonal') added mass coefficients of from 1 to 6 percent; modelling appendage thickness may increase the prediction of $X_{\dot{u}}$ by as much as 30 percent.

If more accuracy than the present theory provides is required, the theory should progress on at least two fronts simultaneously: circulation should be properly accounted for in the flow, so that the added masses become a function of the state variables; and, a better geometrical representation of the multi-component vehicle should be developed. Since added mass is merely a measure of the kinetic energy in the flow, properly accounting for boundary layer growth, separation, and the flow structures they generate, all of which effectively use up or re-distribute kinetic energy, may also be necessary. The effect of the propeller may also need to be considered. Accounting for any of these features would require a major extension of the present theory.

Future work should consider the effect of a free surface on the added masses. As well, sensitivity studies should be carried out in order to establish the accuracy with which the added mass coefficients should be known.

APPENDIX A

Elliptic Functions

This appendix describes methods for evaluating elliptic integrals of the first and second kinds. Extensive use is made of the theory of theta functions and Jacobian elliptic functions, as presented by Whittaker and Watson[11], Chapters 21 and 22, and Watt[13], Appendix B. The serious reader is advised to at least look over Reference 11.

The fundamental elliptic integral of the first kind is:

$$u = \int_0^x \frac{dt}{\sqrt{(1-t^2)(1-k^2t^2)}} = \int_0^\phi \frac{d\theta}{\sqrt{1-k^2\sin^2\theta}} \tag{A1}$$

where k is the modulus of the integral: $0 < k < 1$. These integrals are related through the variable transformation $t = \sin\theta$. If $x = 1$, so that $\phi = \pi/2$, the integral is called a complete elliptic integral of the first kind and is represented by the symbol K. The complementary modulus, $k' \equiv \sqrt{1-k^2}$, determines the only other complete elliptic integral of the first kind, K', which is the same function of k' as K is of k.

The Jacobian elliptic functions $\mathrm{sn}(u,k)$, $\mathrm{cn}(u,k)$, and $\mathrm{dn}(u,k)$ (usually written simply as $\mathrm{sn}\,u$, $\mathrm{cn}\,u$, and $\mathrm{dn}\,u$ if the value of the modulus to be used is k) are related to each other via:

$$\mathrm{sn}^2 u + \mathrm{cn}^2 u = 1\,, \quad \mathrm{dn}^2 u + k^2\,\mathrm{sn}^2 u = 1\,. \tag{A2}$$

Also:

$$\frac{d}{du}\,\mathrm{sn}\,u = \mathrm{cn}\,u\,\mathrm{dn}\,u\,, \quad \frac{d}{du}\,\mathrm{cn}\,u = -\,\mathrm{sn}\,u\,\mathrm{dn}\,u\,, \quad \frac{d}{du}\,\mathrm{dn}\,u = -k^2\,\mathrm{sn}\,u\,\mathrm{cn}\,u\,. \tag{A3}$$

Substituting $t = \mathrm{sn}\,u$ in the integrand of equation A1 gives:

$$u = \mathrm{sn}^{-1}\,x \quad \Longrightarrow \quad x = \mathrm{sn}\,u \tag{A4}$$

so that the inverse sn function can be defined as an incomplete elliptic integral of the first kind. Whereas the trigonometric functions $\sin u$ and $\cos u$ are *singly* periodic in the complex u plane (they are periodic along the real axis but not along the imaginary axis), the Jacobian elliptic functions are *doubly* periodic. For example, $\mathrm{sn}\,u = \mathrm{sn}(u \pm 4mK \pm 2niK')$ for $m, n = 0, 1, 2, \ldots$, leading to cells of periodicity in the complex u plane.

The fundamental elliptic integral of the second kind is:

$$E(u,k) \equiv \int_0^u \mathrm{dn}^2(u,k)\,du \tag{A5}$$

or, making the substitution $t = \mathrm{sn}\,u$, followed by $t = \sin\theta$:

$$E(u) = \int_0^x \sqrt{\frac{1-k^2t^2}{1-t^2}}\,dt = \int_0^\phi \sqrt{1-k^2\sin^2\theta}\,d\theta\,. \tag{A6}$$

When $x = 1$, the integral is designated E (ie, $E \equiv E(K)$) and is called a complete elliptic integral of the second kind. E' is the only other complete elliptic integral of the second kind and it is the same function of k' as E is of k.

When numerical work must be done, the use of theta functions is advised. The Jacobian elliptic functions can be constructed from the four *quasi-doubly* periodic theta functions:

$$\mathrm{sn}(u,k) = \frac{1}{\sqrt{k}}\frac{\vartheta_1(z,q)}{\vartheta_4(z,q)}, \quad \mathrm{cn}(u,k) = \sqrt{\frac{k'}{k}}\frac{\vartheta_2(z,q)}{\vartheta_4(z,q)}, \quad \mathrm{dn}(u,k) = \sqrt{k'}\frac{\vartheta_3(z,q)}{\vartheta_4(z,q)} \tag{A7}$$

where the theta functions are more naturally defined in terms of:

$$z = \frac{\pi}{2K}u. \tag{A8}$$

The parameter q is purely a function of k, and is to the theta functions what k is to the Jacobian elliptic functions:

$$q = e^{-\pi K'/K}. \tag{A9}$$

Whittaker and Watson give:

$$\begin{aligned}
\vartheta_1(z) &= 2q^{\frac{1}{4}}\sin z - 2q^{\frac{9}{4}}\sin 3z + 2q^{\frac{25}{4}}\sin 5z - \cdots \\
\vartheta_2(z) &= 2q^{\frac{1}{4}}\cos z + 2q^{\frac{9}{4}}\cos 3z + 2q^{\frac{25}{4}}\cos 5z + \cdots \\
\vartheta_3(z) &= 1 + 2q\cos 2z + 2q^4\cos 4z + 2q^9\cos 6z + \cdots \\
\vartheta_4(z) &= 1 - 2q\cos 2z + 2q^4\cos 4z - 2q^9\cos 6z + \cdots .
\end{aligned} \tag{A10}$$

Now, if:

$$2\epsilon_0 \equiv \frac{1-\sqrt{k'}}{1+\sqrt{k'}} = \frac{k^2}{\left(1+k'\right)\left(1+\sqrt{k'}\right)^2} \tag{A11}$$

(the latter form of this equation being the most accurate for numerical calculations when k is very small) then Whittaker and Watson show that:

$$q = \epsilon_0 + 2\epsilon_0^5 + 15\epsilon_0^9 + 150\epsilon_0^{13} + O\left(1000\epsilon_0^{17}\right). \tag{A12}$$

$q, \epsilon_0 \to 0$ as $k \to 0$ and $q, 2\epsilon_0 \to 1$ as $k \to 1$. Nevertheless, this equation is accurate for surprisingly large values of k. For complete coverage of the range of k values right through to 1, however, one replaces k' with k in equation A11 and then calculates q' from equation A12. q and q' are related via:

$$q' = e^{-\pi K/K'} = e^{\pi^2/\ln q}. \tag{A13}$$

With q determined, equations A14 and A15 give the complete elliptic integrals of the first and second kinds:

$$\begin{aligned}
\frac{2K}{\pi} &= \left(1 + 2q + 2q^4 + 2q^9 + 2q^{16} + \cdots\right)^2 \\
\frac{2K'}{\pi} &= \frac{-1}{\pi}\left(\frac{2K}{\pi}\right)\ln q \\
\frac{E}{K} &= k'^2 + 8\left(\frac{\pi}{2K}\right)^{5/2}\left(q + 4q^4 + 9q^9 + 16q^{16} + \cdots\right).
\end{aligned} \tag{A14}$$

Legendre's relation gives E':

$$EK' + E'K - KK' = \frac{\pi}{2}. \tag{A15}$$

Of course, if $q' < q$, it would make more sense to calculate K' from the first of equations A14 (replacing q with q'), K from the second, E' from the third, and then E from equation A15. Since $q = q'$ when $k = k'$ and $K = K'$, q or q' need never be larger than $e^{-\pi} = 0.043$ in the above calculations. These procedures, then, give very good accuracy. For greater accuracy, the procedures presented by Watt using series in powers of q^{16} can be used.

The Incomplete Elliptic Integral of the First Kind

The integral of equation A1 can be accurately evaluated using Landen's transformation, a change of variables in the integrand which, when repeated several times, results in an integral which is closely approximated by an elementary function. Although the technique is simple and easy to apply, a different approach will be used here—one which is in keeping with the use of theta functions. This is because Landen's transformation is not readily extended to incomplete elliptic integrals of the second kind, whereas theta functions can handle them easily. The technique presented is at least as accurate and fast as Landen's transformation and becomes more efficient when the other procedures of this appendix must also be calculated.

An important property of the theta functions is that:

$$\begin{aligned} \vartheta_3(z,q) + \vartheta_4(z,q) &= 2\vartheta_3(2z,q^4) \\ \vartheta_3(z,q) - \vartheta_4(z,q) &= 2\vartheta_2(2z,q^4)\,. \end{aligned} \tag{A16}$$

This allows the procedure that produced equations A11 and A12 to be generalized when the Jacobian elliptic functions of u are known. Using the last of equations A7, Watt shows that if:

$$\begin{aligned} 2\epsilon_z \equiv \frac{\mathrm{dn}\,u - \sqrt{k'}}{\mathrm{dn}\,u + \sqrt{k'}} &= \frac{\vartheta_2(2z,q^4)}{\vartheta_3(2z,q^4)} \\ &= \frac{2q\cos 2z + 2q^9\cos 6z + 2q^{25}\cos 10z + \cdots}{1 + 2q^4\cos 4z + 2q^{16}\cos 8z + \cdots} \end{aligned} \tag{A17}$$

then:

$$\cos 2z \sim \frac{\epsilon_z}{q}\left[1 + 2q^4\left(2\cos^2 2z - 1\right) - q^8\left(4\cos^2 2z - 3\right) - \cdots\right].$$

By continually substituting this equation into itself, an asymtotic expansion for $\cos 2z$ in powers of q^4 is obtained in terms of:

$$\varsigma \equiv \frac{\epsilon_z}{q} \tag{A18}$$

is obtained. As $q \to 0$:

$$\cos 2z \sim \varsigma\left[1 - q^4\left(2 - 4\varsigma^2\right) + q^8\left(3 - 20\varsigma^2 + 32\varsigma^4\right) - q^{12}\left(6 - 76\varsigma^2 + 272\varsigma^4 - 320\varsigma^6\right) + O\left(1000q^{16}\right)\right]. \tag{A19}$$

$0 < 2z < \pi$ if $0 < u < K$ (ie, when $0 < x < 1$). Note that z can be real or imaginary. For z real, $|\varsigma| < 1$ and the coefficients of powers of q^4 in equation A19 are no worse then the coefficients of powers of q in the expression for q/ϵ_0, from equation A12.

Equation A19 works well when $q \ll 1$. If not, let:

$$\begin{aligned} 2\epsilon'_z \equiv \frac{\mathrm{dn}(iu,k') - \sqrt{k}}{\mathrm{dn}(iu,k') + \sqrt{k}} &= \frac{\vartheta_2(2z',q'^4)}{\vartheta_3(2z',q'^4)} \\ &= \frac{\mathrm{dn}\,u - \sqrt{k}\,\mathrm{cn}\,u}{\mathrm{dn}\,u + \sqrt{k}\,\mathrm{cn}\,u} \end{aligned} \tag{A20}$$

where use has been made of a manifestation of Jacobi's imaginary transformation:

$$\mathrm{sn}(iu,k') = \frac{i\,\mathrm{sn}(u,k)}{\mathrm{cn}(u,k)}\,, \quad \mathrm{cn}(iu,k') = \frac{1}{\mathrm{cn}(u,k)}\,, \quad \mathrm{dn}(iu,k') = \frac{\mathrm{dn}(u,k)}{\mathrm{cn}(u,k)}\,. \tag{A21}$$

Then, with:

$$x' = \frac{\pi}{2K'}iu\,, \quad \varsigma' \equiv \frac{\epsilon'_x}{q'} \tag{A22}$$

it follows that, as $q' \to 0$:

$$\cosh\left(\frac{\pi}{2K'}2u\right) \sim \varsigma'\Big[1 - q'^4\left(2 - 4\varsigma'^2\right) + q'^8\left(3 - 20\varsigma'^2 + 32\varsigma'^4\right) - q'^{12}\left(6 - 76\varsigma'^2 + 272\varsigma'^4 - 320\varsigma'^6\right) + O\left(1000\varsigma'^8 q'^{16}\right)\Big]. \tag{A23}$$

In the range $0 < u < K$, ς' varies from a minimum of approximately 1 at $u = 0$ to a maximum of $1/2q'$ at $u = K$. Thus, equation A23 will not be as accurate as its counterpart, equation A19; however, between the two of them, the complete range of k values can be accurately covered.

The Incomplete Elliptic Integral of the Second Kind

Whittaker and Watson show that the incomplete elliptic integral of the second kind can be written:

$$E(u) = u\,\frac{E}{K} + \frac{\pi}{2K}\frac{\vartheta'_4(z)}{\vartheta_4(z)} \tag{A24}$$

where $\vartheta'_4(z)$ is the derivative of $\vartheta_4(z)$ with respect to z. This expression can now be evaluated using equations A10. However, there is a more efficient and accurate method available.

By taking the derivative of the logarithm of the first of equations A16 and the last of equations A7, Watt shows that:

$$\frac{\vartheta'_4(z)}{\vartheta_4(z)} = \frac{2K}{\pi}\,\frac{k^2\,\mathrm{sn}\,u\,\mathrm{cn}\,u}{\mathrm{dn}\,u + \sqrt{k'}} + 2\frac{\vartheta'_3(2z,q^4)}{\vartheta_3(2z,q^4)}\,. \tag{A25}$$

Thus, if the Jacobian elliptic functions of u are known, the number of terms that need to be evaluated in a calculation of $E(u)$ can be substantially reduced. This is particularly true if u is imaginary, as in the next paragraph.

Equation A25 works well if $q \ll 1$. If it is not, another form of Jacobi's imaginary transformation can be exploited:

$$E(u) = u + \frac{\mathrm{sn}\,u\,\mathrm{dn}\,u}{\mathrm{cn}\,u} + iE(iu,k')\,. \tag{A26}$$

$E(iu,k')$ is then expanded in a manner analogous to equation A24:

$$E(iu,k') = iu\frac{E'}{K'} + \frac{\pi}{2K'}\frac{\vartheta'_4(x',q')}{\vartheta_4(x',q')}\,. \tag{A27}$$

Hence, for $q' \ll 1$:

$$E(u) = u\left(1 - \frac{E'}{K'}\right) + \frac{\mathrm{sn}\,u\left(k^2\,\mathrm{cn}\,u + \sqrt{k}\,\mathrm{dn}\,u\right)}{\mathrm{dn}\,u + \sqrt{k}\,\mathrm{cn}\,u} + 2i\frac{\pi}{2K'}\frac{\vartheta'_3(2z',q'^4)}{\vartheta_3(2z',q'^4)}\,. \tag{A28}$$

APPENDIX B

Program ESAM User Instructions

This appendix gives the user instructions and describes the data input and output formats for ESAM (Estimate Submarine Added Masses), a FORTRAN 77 program which performs the calculations required by the theory developed in the main body of this report. After compiling, linking, and running the program, the user is asked to give the name of the input file which must contain all the data for a complete run. The user simply enters this file name; except for possible error messages being written to the designated output unit (the terminal on a VAX), there is no other interaction with the user. Output is sent to a newly created file, ESAM.OUT. If for some reason the program terminates, ESAM.OUT will show how many components were successfully processed before termination occurred. If an error message is written to the screen by ESAM, it will also be written to ESAM.OUT.

B.1 Input Format

This section describes the data (and the order in which they must occur) that the input file must contain. In general, data should appear exactly as specified in the input format summary; spaces should not be left between lines. However, since READ statements in ESAM are free format (except for those reading character constants), numerical data can be split between different lines if desired. ESAM does its best to test the input data to make sure the rules described below are being followed; if they are not, an appropriate error message is given.

Input format summary

```
NC
XDIR
XOFF
ZOFF
ELL
TYPE COMMENT
XSHIFT,YSHIFT,ZSHIFT        } Optional; may replace with /.
N
XO,B(XO),H(XO),HBAR(XO)     } Only need to enter X1,B(X1) if profile is designated axiSymmetric.
X1,B(X1),H(X1),HBAR(X1)     }                                  } assuming type is H.
        :                   }
XN,B(XN),H(XN),HBAR(XN)     }
TYPE COMMENT
X1,Y1,Z1,PHI,XH2,YH2,XH3,YH3,XH4,YH4,T                         } assuming type is 1 or 2.
TYPE COMMENT
X1,Y1,Z1,PHI,C1,XH4,YH4,C4,XH5,YH5,C5,T                        } assuming type is 3.
TYPE COMMENT
A,B,C,XBAR,YBAR,ZBAR,PHI,OMEGA                                 } assuming type is E.
  :
```

Various TYPEs of components are added to this list, as required.

Definition of variables

NC — An integer specifying the number of components which make up the submarine and for which data is about to be specified. Array dimensioning limits NC to, at most, 20.

XDIR — The added mass coefficients output from this program are *always* calculated relative to the conventional body fixed system of axes used by the DTNSRDC standard submarine equations of motion[8]. Although, in general, this will also be the coordinate system used to input submarine geometry, provision is made for input data x coordinates that increase opposite to the standard sense. Note that all data input during a run of the program must be referenced to an identical set of input axes, whatever they may be.

XDIR is a character specifying the direction of increasing x for all input data: if XDIR is P (for positive), the coordinate system for the input data will be the standard body fixed system of axes, with x coordinates increasing from stern to bow; if XDIR is N (for negative), the input coordinate system will still be the standard body axes except that the x direction will be reversed so that x coordinates increase from bow to stern (y and z coordinates always increase going to starboard and going downwards, respectively, regardless of XDIR being P or N).

The summary of geometrical information written to ESAM.OUT is also converted to the standard axes used by the added mass coefficients. The next paragraph specifies how the origin of this system is determined.

XOFF
ZOFF — All data must be input relative to the same origin, which can be located anywhere that is convenient. XOFF and ZOFF (x-offset and z-offset) are real constants that are subtracted from the input x and z coordinates to give a new origin for the body fixed axes to which all output is referenced. Note that the input and output data have identical y axis origins.

Sometimes it is desirable to locate the output axes origin at the center of bouyancy, even though knowledge of its location is unknown beforehand. Although ESAM does not accurately calculate this point, the location of the centroid of the replacement hull ellipsoid closely approximates it. If the user wishes to use either or both of the x and z coordinates of this location for specifying his output origin, he need only input C (for centroid) for either or both of XOFF and ZOFF. If this is done, the centroid of the first component entered locates the new origin, so this first component must represent the hull.

ELL — A real constant equal to the hull length; its magnitude is used to nondimensionalize the added mass coefficients. If ELL = 0, nondimensionalization does not take place; in this case, the added masses need only be multiplied by the fluid density (in units consistent with those of the input data) to obtain the actual added masses.

ELL is also used to determine the format in which the added mass coefficients are written to ESAM.OUT: if ELL is greater than zero, the coefficients are written via the edit descriptor F15.10; if ELL is less than or equal to zero, the descriptor 1PE15.8 is used. Thus, the user chooses either F or E formatted output for nondimensionalized coefficients by making ELL positive or negative. Dimensional coefficients are always output in E format.

Subsequent records contain component information. The rules given below will determine the order in which some components should be entered.

TYPE This is a character constant of length 2 and it precedes the input format for all TYPEs of components. The first character specifies the component *type*. Component *types* are:

H (for Hull),
1 (for type I appendage),
2 (for type II appendage),
3 (for type III appendage), and
E (for Ellipsoid).

The second character specifying the TYPE is the *order*. It is used to determine if interference effects are to be accounted for on this component. There are 3 *orders*:

P (for Primary),
S (for Secondary), and
N (for Neutral).

A primary component can only be of *type* H or E; it determines the interference velocity field at all secondary components entered between it and the next primary component; its added masses are not corrected for interference effects from any other component. Although ESAM does not prevent the user from entering more than one primary component, to do so makes little sense since it implies more than one independent configuration is being processed at once, and ESAM sums all the component added masses into one total added mass.

A secondary component can be associated with any *type*; it must be preceded by a primary component.

A neutral component can also be associated with any *type*; it has no effect on any other component; it is not corrected for interference effects; it can be entered anywhere amongst the other components.

There can be any number of primary, secondary, and neutral *order* components during a run, up to a total of 20 (limited only by array dimensioning). Of course, primary and secondary components must be ordered in a meaningful way.

Examples of various TYPEs are: HP, HS, HN, 1S, 3N, and EP. The first 3 component designations, here, indicate hull components which are of primary, secondary, and neutral *orders*, respectively. The fourth component is a *type* 1 appendage of secondary *order*. The fifth is a *type* 3 appendage of neutral *order*. The last one specifies an ellipsoid of primary *order*.

COMMENT A character constant of length 12; it must be on the same line as TYPE and separated from it by 2 characters. COMMENT is any phrase the user wants to use to describe the associated component; it is only used for descriptive purposes in ESAM.OUT, and may be left blank. Actually, ESAM reads in 'TYPE COMMENT' as a single constant of length 16.

If the TYPE designation specifies *type* H, then Φ and Ω are set to zero and the following input format must follow TYPE, regardless of the *order*:

XSHIFT,YSHIFT,ZSHIFT — Real constants specifying, in the usual input coordinate system, a shift to be applied to the hull component coordinates. XSHIFT and ZSHIFT are effectively added to the values of Xi and HBAR(Xi) defined below. $\bar{y}$ is equated to YSHIFT. Although these data are unnecessary for a primary hull component, which can make use of the XOFF and ZOFF inputs and for which $\bar{y}$ is invariably zero, they are convenient for secondary components which are not hulls but instead are pods or some other cylindrical type of body mounted out from the hull. If the shift coordinates are used with a primary component, one should ensure that subsequent secondary components are properly positioned relative to the shifted primary component; unlike XOFF and ZOFF, the shift coordinates are only applied to the hull component they are associated with.

Since use of the shift coordinates will usually be unnecessary, this record may be bypassed, in the usual way for list directed input, by replacing it with a /. Bypassing the record is equivalent to setting the shift coordinates to zero.

N — An integer specifying the number of sections the component is divided into for the purposes of numerically specifying its profile. Note that N sections are delineated by N + 1 stations and that profile coordinates must be given at each station. Array dimensioning restricts N to being less than or equal to 100.

XO,B(XO),H(XO),HBAR(XO)
X1,B(X1),H(X1),HBAR(X1)
⋮
XN,B(XN),H(XN),HBAR(XN)

Here, Xi is the x coordinate of the i^{th} axial station; it must not decrease as its index increases. Xi will increase from stern to bow if XDIR is positive and from bow to stern if XDIR is negative.

B(Xi) is the hull component's local breadth; it is assumed to be symmetrical about $y = \bar{y}$.

H(Xi) is the local height as seen in a sheer plan; it is not assumed to be symmetrical in any sense.

HBAR(Xi) is the x coordinate of the mid-point of the local height, H(Xi). HBAR(Xi) can be used to describe two things: 1) the "camber" of the elevation profile and 2) the height of the component above or below the input x axis. Although this latter capability allows the component to be raised or lowered relative to the input x axis, the simplest way to do this is to use ZSHIFT.

Note that the N + 1 stations need *not* be evenly distributed over the hull component. Profile coordinates can be concentrated in areas of high curvature, such as the nose, and eliminated from regions of zero curvature (ie, where the breadth and sheer profiles are straight lines). This is because the only approximation made in the numerical integration of the integrals of equations 74 and 83 is that the input profile coordinates are all joined by straight lines; if in fact they are, then the integrals are evaluated exactly. Thus, a hull component with a long cylindrical mid-body section, for example, only needs to have the mid-section profile specified at its endpoints.

For axisymmetric profiles, only Xi,B(Xi) need be entered. However, ESAM must first be told that this will be the case; this is done by appending an S (for axiSymmetric) to the TYPE. For an axisymmetric hull component of primary *order*,

'TYPE COMMENT' might look like 'HPS HULL ', with only 1 character separating HPS and HULL. For the axisymmetric case, ESAM always looks for X1,B(X1) at the beginning of a new record. Thus, if a user wants to specify an axisymmetric hullform using an asymmetric data file, deletion of the H(X1),HBAR(X1) data is unnecessary if it is on the same lines as the X1,B(X1) data. Designating the hull component as axisymmetric has two other minor consequences: 1) ESAM's calculations will be a little quicker, since certain simplifications can be made; 2) the errors specifying the accuracy with which the replacement ellipsoid is able to model the true hull component are not written to ESAM.OUT, since they are always zero for an axisymmetric profile.

It is permissible to input axisymmetric hull components using the asymmetric format.

This completes the hull component input data. Now, the input file will either terminate or the next entry will be another TYPE variable, followed by its associated component information.

If the TYPE designation specifies a *type* 1 or 2 appendage, then the following input format must follow TYPE. The user is reminded that the only difference between a *type* 1 and 2 appendage is in how the sweepback angle, Ω, is calculated: for *type* 1, Ω equals the sweepback angle of the bisector of the angle formed by the leading and trailing edges; for *type* 2, Ω is the angle between the line joining the leading and trailing edge root coordinates and the body x axis.

X1,Y1,Z1,PHI,XH2,YH2,XH3,YH3,XH4,YH4,T — These are all real constants. Because of the free format READ statement, they can be entered on different lines if the user wishes.

X1,Y1,Z1 are the coordinates of the appendage trailing edge at the root, using the usual input coordinate system.

PHI is the angle Φ (in degrees) the y axis must rotate about the x axis to bring it into the plane of the control surface; for a sail, for example, PHI could be input as -90 or 270.

XH2,YH2 are the coordinates $(\hat{x}_2, \hat{y}_2)$ of the leading edge at the root, using an unswept local coordinate system with its origin at (X1,Y1,Z1), the XH axis pointing towards the bow (parallel to the body x axis), the YH axis pointing outwards towards the appendage tip, and with the ZH axis perpendicular to the planform of the appendage (see the text, Figure 2).

XH3,YH3 are the local coordinates $(\hat{x}_3, \hat{y}_3)$ of the leading edge at the tip.

XH4,YH4 are the local coordinates $(\hat{x}_4, \hat{y}_4)$ of the trailing edge at the tip.

T is the thickness to chord ratio, t, of the section profile.

Note that *triangles* can be input in this format. If (XH3,YH3) is coincident with (XH4,YH4), processing continues normally. If (XH2,YH2) is coincident with (XH3,YH3) or if (XH4,YH4) is coincident with (0,0), then the appendage is automatically converted to a *type* 2 appendage, if it isn't already, so that Ω is taken to be the argument of the (XH2,YH2) vector.

This completes the *type* 1 and 2 appendage component input data. Now, the input file will either terminate or the next entry will be another TYPE variable, followed by its associated component information.

If the TYPE designation specifies a *type* 3 appendage, then the following input format must follow TYPE. The user is reminded that the sweepback angle, Ω, is taken to be zero for this appendage. As noted in the text, a pair of appendages separated by the hull should not be represented with a *type* 3 appendage if one wishes to account for interference effects.

X1,Y1,Z1,PHI,C1,XH4,YH4,C4,XH5,YH5,C5,T — These are all real constants; they can be entered on different lines if the user wishes.

X1,Y1,Z1 are the coordinates of the appendage trailing edge at the root, using the usual input coordinate system.

PHI is the angle Φ (in degrees) the y axis must rotate about the x axis to bring it into the plane of the control surface; for a sail, for example, PHI could be input as -90 or 270.

C1 is the root chord length c_1, assumed parallel to the body x axis.

XH4,YH4 are the coordinates $(\hat{x}_4, \hat{y}_4)$ of the trailing edge at the upper tip, using an unswept local coordinate system with its origin at (X1,Y1,Z1), the XH axis pointing towards the bow (parallel to the body x axis), the YH axis pointing towards the upper tip, and with the ZH axis perpendicular to the planform of the appendage.

C4 is the upper tip chord length c_4, parallel to the body x axis.

XH5,YH5 are the local coordinates $(\hat{x}_5, \hat{y}_5)$ of the trailing edge at the lower tip (so YH5 will be negative).

C5 is the lower tip chord length c_5, parallel to the body x axis.

T is the thickness to chord ratio, t, of the section profile.

In this discussion, the terms 'upper' and 'lower' tip were used to orient the reader. These are really misnomers, however, since PHI can be used to rotate the planform to any desired angle.

This completes the *type* 3 appendage component input data. Now, the input file will either terminate or the next entry will be another TYPE variable, followed by its associated component information.

If the TYPE designation specifies a *type* E component, then the following input format must follow TYPE. This component is an ellipsoid which the user can place anywhere he likes. Since it is already an exact ellipsoidal representation of itself, ESAM does not replace it with any other geometry. If this component is of primary *order*, then PHI and OMEGA must be zero.

A,B,C,XBAR,YBAR,ZBAR,PHI,OMEGA — These are all real constants; they can be entered on different lines if the user wishes.

A,B,C are the ellipsoid principal semi-axis lengths a, b, c: A is associated with the x' axis (the x axis if OMEGA $= 0$), B with the y' axis (the y axis if PHI $=$ OMEGA $= 0$), and C with the z' axis (the z axis if PHI $=$ OMEGA $= 0$).

XBAR,YBAR,ZBAR are the coordinates, using the usual input data coordinate system, of the ellipsoid's centroid.

PHI,OMEGA are the angles Φ and Ω (in degrees) defining the orientation of the ellipsoid principal axes relative to the body fixed axes: PHI is the angle the y' axis has rolled away from the y axis; after applying this roll, OMEGA is the angle the x' axis pitches up from the x axis; positive angular deflections are defined using the Right Hand Rule. These angles are thoroughly discussed in Section 2 of the text.

This completes the *type* E component input data. Now, the input file will either terminate or the next entry will be another TYPE variable, followed by its associated component information.

Example input format

The data shown below is a listing of the input file for the generic submarine described in Section 10 of the text. The input data origin is implicitly defined as the nose of the submarine by XDIR, the setting of the hull shift coordinates to zero, and the first line of the hull profile data. Note that commenting text in the data file, other than the COMMENT input, is not read since ESAM will have finished reading the record before getting to it.

```
8           # of components making up the submarine.
n           Input data x-coordinate increases going from bow to stern.
c           Output data x-axis origin is opposite centroid of ellipsoid 1.
0.0         Output data z-axis origin is coincident with input origin.
453.            Hull length used for nondimensionalization.
hp  HULL        Component 1 is a hull component of primary 'order'.
/               shift coordinates are set to zero.
23              # sections => 24 stations.
0.      0.      0.      0.
1.      5.7     8.      0.02
2.      9.      11.2    .04
4.      12.     16.1    .08
8.5     17.4    21.5    .17
17.     22.7    27.4    .35
25.     26.2    31.2    .51
35.     30.7    33.7    .72
73.     38.1    39.7    1.5
97.     39.6    41.4    1.25
102.    40.     42.1    .9
108.    40.4    44.2    0.
158.    42.5    49.9    -2.5
267.    40.     49.6    -2.7
290.    38.4    49.4    -2.8
299.    37.7    46.9    -2.
310.    36.4    42.9    -.5
313.    36.     40.6    .2
317.    35.6    37.4    1.7
353.    29.9    32.9    .75
388.    21.2    24.9    .6
410.    14.9    18.2    0.
440.    6.5     6.8     0.
453.    0.      0.      0.
1s  SAIL          COMPONENT 2
158.,0.,-27.5       -90.        50.,-5.4    50.,26.1    3.,26.1     .3
1s  STBD SAILPLN            3
129.,7.73,-40.1       0.        20.5,-2.02  15.5,15.    6.0,15.     .15
1s  PORT SAILPLN            4
129.,-7.73,-40.1    180.        20.5,-2.02  15.5,15.    6.0,15.     .15
```

```
1s  TOP RUDDER              5
440.,0.,-3.4        -90.        17.65,4.02    14.35,18.    0.,18.      .15
1s  BOT RUDDER              6
440.,0.,3.4          90.        17.65,4.02    14.35,18.    0.,18.      .15
1s  STBD STRNPLN            7
443.,3.,0.            0.        29.,4.1       19.,22.3     8.,22.3     .15
1s  PORT STRNPLN            8
443.,-3.,0.         180.        29.,4.1       19.,22.3     8.,22.3     .15
```

B.2 Output Format

The output file (ESAM.OUT) containing the output from a run using the above input is shown on the next page. It uses a full 132 character line.

Interpreting this output file is, for the most part, straightforward. Except for the listing of XOFF and ZOFF in line 5, all output is specified relative to the standard body fixed system of axes. The section giving the 'EQUIVALENT ELLIPSOID REPLACEMENT GEOMETRY' may need some explanation. Ignoring the last line and the lines beginning with 'Optmzd comp...', this section is simply listing the characteristics of the replacement ellipsoids for the specified components. These characteristics determine the added masses of a component, neglecting interference effects. The last line of the section gives the errors associated with fitting the asymmetyric hull with a single ellipsoid, as defined in Section 8 of the text by equations 85 and, for EXbar, equation 77; this line is not printed for a hull component which is designated axisymmetric, nor for one of secondary *order*.

If a component is of secondary *order*, then interference effects are determined by the velocity field around the replacement ellipsoid of its associated primary component. However, if the primary component is of *type* H, this replacement ellipsoid geometry is first optimized to reflect more accurately the local hull component geometry opposite the x location of the secondary ellipsoid's centroid. It is this primary ellipsoid optimized geometry that the lines beginning 'Optmzed comp ...' are listing; only changes to the original replacement ellipsoid geometry are noted in this row. This optimized geometry is only used for calculating the interference velocities for the secondary component of the previous line; it has no effect on the added masses of any other component, including the primary component itself. If the primary component is of *type* E, no optimization takes place.

ESAM.OUT, output file from PROGRAM ESAM on 7-JAN-88 at 08:24:47 hrs.
The input file is: egw.INP
A 8 component body.
Input data x direction was OPPOSITE TO the conventional x direction to which all output is referenced: XDIR = NEGATIVE
Relative to the input coordinate system, the output coordinate system's origin is located at: x = 200.202253, z = 0.000000

EQUIVALENT ELLIPSOID REPLACEMENT GEOMETRY

comp	type	a	b	c	Xbar	Ybar	Zbar	Phi	Omega	component
1	hp	217.921999	21.562767	24.653845	0.000000	0.000000	-1.197562	0.000000	0.000000	HULL
2	ls	26.154709	18.096138	7.846413	68.313343	0.000000	-38.860128	-90.000000	-3.278473	SAIL
Optmzd comp	1:		21.800498	24.706997			-1.194446			
3	ls	8.540274	9.513390	1.281041	81.671370	12.943086	-40.100000	0.000000	-2.715048	STBD SAILPLN
Optmzd comp	1:		22.026520	24.484800			-0.526544			
4	ls	8.540274	9.513390	1.281041	81.671370	-12.943086	-40.100000	180.000000	-2.715048	PORT SAILPLN
Optmzd comp	1:		22.026520	24.484800			-0.526544			
5	ls	8.713415	9.967470	1.307012	-231.890937	0.000000	-12.841661	-90.000000	6.640816	TOP RUDDER
Optmzd comp	1:	243.737747	14.147216	15.917960			0.000000			
6	ls	8.713415	9.967470	1.307012	-231.890937	0.000000	12.841661	90.000000	6.640816	BOT RUDDER
Optmzd comp	1:	243.737747	14.147216	15.917960			0.000000			
7	ls	11.707658	11.587330	1.756149	-228.701180	12.488846	0.000000	0.000000	4.525727	STBD STRNPLN
Optmzd comp	1:	243.737747	13.891053	15.929310			0.000000			
8	ls	11.707658	11.587330	1.756149	-228.701180	-12.488846	0.000000	180.000000	4.525727	PORT STRNPLN
Optmzd comp	1:	243.737747	13.891053	15.929310			0.000000			

Comp 1 hull fit Errs (rltve to TOTALS): EYvd,EZwd= -1.2% 1.3%; EKpd,EMqd,ENrd= -2.2% -1.2% 1.2%; EXbar= 0.5% of hull length.

THE DIMENSIONLESS ADDED MASSES; the nondimensionalizing length is: 453.000000

component	type	Xud	Xvd,Yud	Xwd,Zud	Xpd,Kud	Xqd,Mud	Xrd,Nud	Nrd
HULL	hp	-0.0002358136	0.0000000000	0.0000000000	0.0000000000	0.0000006234	0.0000000000	-0.0004884119
SAIL	ls	-0.0000599978	0.0000000000	-0.0000019048	0.0000000000	0.0000040164	0.0000000000	-0.0000209217
STBD SAILPLN	ls	-0.0000011090	-0.0000001117	-0.0000007025	-0.0000000232	0.0000002017	0.0000000049	-0.0000000749
PORT SAILPLN	ls	-0.0000011090	0.0000001117	-0.0000007025	0.0000000232	0.0000002017	-0.0000000049	-0.0000000749
TOP RUDDER	ls	-0.0000011269	0.0000000000	0.0000001929	0.0000000000	0.0000001248	0.0000000000	-0.0000152586
BOT RUDDER	ls	-0.0000011269	0.0000000000	-0.0000001929	0.0000000000	-0.0000001248	0.0000000000	-0.0000152586
STBD STRNPLN	ls	-0.0000022848	-0.0000003977	0.0000000000	0.0000000000	0.0000002485	0.0000000000	-0.0000004438
PORT STRNPLN	ls	-0.0000022848	0.0000003977	0.0000000000	0.0000000000	0.0000000000	-0.0000002485	-0.0000004438
TOTALS:		-0.0003048529	0.0000000000	-0.0000033097	0.0000000000	0.0000050433	0.0000000000	-0.0005408884

component	type	Yvd	Ywd,Zvd	Ypd,Kvd	Yqd,Mvd	Yrd,Nvd	Mpd	Mrd,Nqd
HULL	hp	-0.0114114467	0.0000000000	-0.0000301676	0.0000000000	0.0000000000	-0.0003725955	0.0000000000
SAIL	ls	-0.0009706864	0.0000000000	-0.0000621166	0.0000000000	-0.0001417905	-0.0000012774	0.0000000000
STBD SAILPLN	ls	-0.0000024991	-0.0000056130	-0.0000002982	0.0000010018	-0.0000004312	-0.0000008088	0.0000001677
PORT SAILPLN	ls	-0.0000024991	0.0000056130	-0.0000002982	-0.0000010018	-0.0000004312	-0.0000008088	-0.0000001677
TOP RUDDER	ls	-0.0000596978	0.0000000000	-0.0000014647	0.0000000000	0.0000301792	-0.0000002055	0.0000000000
BOT RUDDER	ls	-0.0000596978	0.0000000000	0.0000014647	0.0000000000	0.0000301792	-0.0000002055	0.0000000000
STBD STRNPLN	ls	-0.0000017320	0.0000000000	0.0000000000	0.0000000000	0.0000008758	-0.0000292393	0.0000000000
PORT STRNPLN	ls	-0.0000017320	0.0000000000	0.0000000000	0.0000000000	0.0000008758	-0.0000292393	0.0000000000
TOTALS:		-0.0125099908	0.0000000000	-0.0000928806	0.0000000000	-0.0000805430	-0.0004343801	0.0000000000

component	type	Zwd	Zpd,Kwd	Zqd,Mwd	Zrd,Nwd	Kpd	Kqd,Mpd	Krd,Npd
HULL	hp	-0.0087405776	0.0000000000	0.0000000000	0.0000000000	-0.0000002730	0.0000000000	0.0000000000
SAIL	ls	-0.0000452823	0.0000000000	0.0000068306	0.0000000000	-0.0000040447	0.0000000000	-0.0000090655
STBD SAILPLN	ls	-0.0000249664	-0.0000009367	0.0000044738	-0.0000009489	-0.0000000437	0.0000001676	-0.0000000510
PORT SAILPLN	ls	-0.0000249664	0.0000009367	0.0000044738	0.0000009489	-0.0000000437	-0.0000001676	-0.0000000510
TOP RUDDER	ls	-0.0000007759	0.0000000000	-0.0000003987	0.0000000000	-0.0000000388	0.0000000000	0.0000007405
BOT RUDDER	ls	-0.0000007759	0.0000000000	-0.0000003987	0.0000000000	-0.0000000388	0.0000000000	-0.0000007405
STBD STRNPLN	ls	-0.0001173051	-0.0000027693	-0.0000585581	0.0000000000	-0.0000000726	-0.0000013824	0.0000000000
PORT STRNPLN	ls	-0.0001173051	0.0000027693	-0.0000585581	0.0000000000	-0.0000000726	0.0000013824	0.0000000000
TOTALS:		-0.0090719548	0.0000000000	-0.0001021354	0.0000000000	-0.0000046281	0.0000000000	-0.0000091675

References

1. Watt, G.D. "Estimates for the Added Mass of a Multi-Component, Deeply Submerged Vehicle." Proceedings, RINA International Symposium on 'Conventional Naval Submarines', May 1988.

2. Lamb, H. **Hydrodynamics.** Cambridge, 6th edition, 1953.

3. Imlay, F.H. "The Complete Expressions for "Added Mass" of a Rigid Body Moving in an Ideal Fluid." DTMB Report 1528, July 1961.

4. Humphreys, D.E. and Watkinson, K.W. "Prediction of Acceleration Hydrodynamic Coefficients for Underwater Vehicles from Geometric Parameters." Naval Coastal Systems Laboratory TR–327–78, February 1978.

5. Aucher, M. "Dynamique des Sous-Marins." Sciences et Techniques de l'Armement, **55**, 4e fascicule 1981.

6. Hooft, J.P. Private Communication.

7. Abkowitz, M.A. **Stability and Motion Control of Ocean Vehicles.** Massachusettes Institute of Technology Press, 1969.

8. Feldman, J. "DTNSRDC Revised Standard Submarine Equations of Motion." DTNSRDC/SPD–0393–09, June 1979.

9. Goldstein, H. **Classical Mechanics.** Addison-Wesley Publishing Co., 1950.

10. Munk, M.M. "The Aerodynamic Forces on Airship Hulls." NACA Report No. 184, 1923.

11. Whittaker, E.T. and Watson, G.N. **A Course of Modern Analysis.** Cambridge University Press, 4th edition, 1927.

12. Munk, M.M. **Aerodynamic Theory.** W.F. Durand editor-in-chief, vol. I, 1934.

13. Watt, G.D. "Multi-Element Thin Airfoil Theory." Ph.D. thesis, University of British Columbia, December 1984.

Unclassified

SECURITY CLASSIFICATION OF FORM
(highest classification of Title, Abstract, Keywords)

DOCUMENT CONTROL DATA

(Security classification of title, body of abstract and indexing annotation must be entered when the overall document is classified)

1. ORIGINATOR (the name and address of the organization preparing the document. Organizations for whom the document was prepared, e.g. Establishment sponsoring a contractor's report, or tasking agency, are entered in section 8.)

Defence Research Establishment Atlantic

2. SECURITY CLASSIFICATION (overall security classification of the document. including special warning terms if applicable)

Unclassified

3. TITLE (the complete document title as indicated on the title page. Its classification should be indicated by the appropriate abbreviation (S,C,R or U) in parentheses after the title.)

ESTIMATES FOR THE ADDED MASS OF A MULTI-COMPONENT, DEEPLY SUBMERGED VEHICLE, PART I: THEORY AND PROGRAM DESCRIPTION

4. AUTHORS (Last name, first name, middle initial. If military, show rank, e.g. Doe, Maj. John E.)

Watt, George D.

5. DATE OF PUBLICATION (month and year of publication of document)	6a. NO. OF PAGES (total containing information. Include Annexes, Appendices, etc.)	6b. NO. OF REFS (total cited in document)
October 1988	60	13

6. DESCRIPTIVE NOTES (the category of the document, e.g. technical report, technical note or memorandum. If appropriate, enter the type of report, e.g. interim, progress, summary, annual or final. Give the inclusive dates when a specific reporting period is covered.)

DREA Technical Memorandum

8. SPONSORING ACTIVITY (the name of the department project office or laboratory sponsoring the research and development. Include the address.)

Defence Research Establishment Atlantic

9a. PROJECT OR GRANT NO. (if appropriate, the applicable research and development project or grant number under which the document was written. Please specify whether project or grant)	9b. CONTRACT NO. (if appropriate, the applicable number under which the document was written)
1AE	

10a. ORIGINATOR'S DOCUMENT NUMBER (the official document number by which the document is identified by the originating activity. This number must be unique to this document.)	10b. OTHER DOCUMENT NOS. (Any other numbers which may be assigned this document either by the originator or by the sponsor)
DREA TECH MEMORANDUM 88/213	

11. DOCUMENT AVAILABILITY (any limitations on further dissemination of the document, other than those imposed by security classification)

(X) Unlimited distribution
( ) Distribution limited to defence departments and defence contractors; further distribution only as approved
( ) Distribution limited to defence departments and Canadian defence contractors; further distribution only as approved
( ) Distribution limited to government departments and agencies; further distribution only as approved
( ) Distribution limited to defence departments; further distribution only as approved
( ) Other (please specify):

12. DOCUMENT ANNOUNCEMENT (any limitation to the bibliographic announcement of this document. This will normally correspond to the Document Availability (11). However, where further distribution (beyond the audience specified in 11) is possible, a wider announcement audience may be selected.)

Unclassified

SECURITY CLASSIFICATION OF FORM

DCD03 2/06/87

Unclassified

SECURITY CLASSIFICATION OF FORM

13. ABSTRACT (a brief and factual summary of the document. It may also appear elsewhere in the body of the document itself. It is highly desirable that the abstract of classified documents be unclassified. Each paragraph of the abstract shall begin with an indication of the security classification of the information in the paragraph (unless the document itself is unclassified) represented as (S), (C), (R), or (U). It is not necessary to include here abstracts in both official languages unless the text is bilingual).

An analytic method is presented for estimating all the added mass terms of a deeply submerged, submarine-like, rigid body. This body may consist of any number of components (hull, sail, fins, etc.). Each component is represented by an ellipsoid with three independently sized principal axes; this allows the added masses to be calculated analytically. Ellipsoid geometry, orientation, and relative location are chosen so that both added masses and added moments of inertia are optimally modelled. Interference effects between the main hull component and an appendage are approximately accounted for by using the flow field around a replacement ellipsoid for the hull to modify the flow at the appendage; interference effects between appendages are neglected. The analysis uses incompressible potential flow theory. It does not account for any circulation in the flow.

Calculations carried out using this method are very fast. They show that both appendage thickness and hull interference can appreciably affect those added mass coefficients which contribute to coupling. Keywords: Submarines hydrodynamics;

14. KEYWORDS, DESCRIPTORS or IDENTIFIERS (technically meaningful terms or short phrases that characterize a document and could be helpful in cataloguing the document. They should be selected so that no security classification is required. Identifiers, such as equipment model designation, trade name, military project code name, geographic location may also be included. If possible keywords should be selected from a published thesaurus, e.g. Thesaurus of Engineering and Scientific Terms (TEST) and that thesaurus-identified. If it is not possible to select indexing terms which are Unclassified, the classification of each should be indicated as with the title.)

Submarine Hydrodynamics
Potential Flow;
Added Mass;
Acceleration Coefficients;
Dynamic Derivatives;
Equations of Motion. Canada (edc)

Unclassified

SECURITY CLASSIFICATION OF FORM